

1

AD-A273 864



AFIT/GAP/ENP/93D-02

HIGH RESOLUTION FOURIER TRANSFORM
ABSORPTION SPECTRUM
OF $^{79}\text{Br}_2$ $\text{B}^3\Pi(0_u^+) \leftarrow \text{X}^1\Sigma_g^+$

THESIS

Robert E. Franklin

Captain, USAF

AFIT/GAP/ENP/93D-02

93-30490

DTIC
ELECTE
DEC 16 1993
S E D

Approved for public release; distribution unlimited

93 12 151 08

HIGH RESOLUTION FOURIER TRANSFORM ABSORPTION

SPECTRUM OF $^{79}\text{Br}_2$ $B^3\Pi(0_u^+) \leftarrow X^1\Sigma_g^+$

THESIS

Presented to the Faculty of the Graduate School of Engineering

of the Air Force Institute of Technology

Air University

In Partial Fulfillment of the

Requirements for the Degree of

Master of Science in Engineering Physics

Robert E. Franklin

Captain, USAF

September 1993

Accession For	
NTIS	CRA&I <input checked="" type="checkbox"/>
DTIC	TAB <input type="checkbox"/>
Unannounced	<input type="checkbox"/>
Justification	
By	
Distribution /	
Availability Codes	
Dist	Avail and/or Special
A-1	

Approved for public release; distribution unlimited

Preface

This research is an investigation into the rovibrational spectrum of diatomic bromine. The last reported high resolution spectroscopy done on the X to B absorption spectrum of this molecule was accomplished over 20 years ago and was done with grating instruments. This effort allowed an experiment to be set up from scratch using current state of the art technology. The prime data gathering instrument, a Fourier Transform Spectrometer, had been received by the department less than 2 months prior to the commencement of this research. I found this work to be gratifying because I was allowed to build this experiment up from nothing and was able to see a plan come together before my eyes. I also found it challenging because so much theory had to be not only learned, but understood.

I would like to thank Major Glen P. Perram, my advisor, for giving me the opportunity to break in his new piece of lab equipment. His support, encouragement, and forever open door policy was greatly appreciated. Also, Dr. Won Roh provided help on theory when it was needed. Thanks also go to Captain Rob Johnson who was my resident Fortran expert when things were bleak in the cold, sterile room upstairs. Finally, I owe a great big hug to my wife. Her patience with me this past summer during the long days and even longer nights was truly amazing. She's always there to remind of where life's priorities need to be.

Robert E. Franklin

Table of Contents

Preface	i
Table of Contents	ii
List of Figures	v
List of Tables	vi
Abstract	vii
I. Introduction	1
Overview	1
Background	2
Problem Statement	2
Summary of Current Knowledge	3
Scope	4
Summary	6
II. Theory	7
Diatomic Molecules	7
Dunham Expansion	8
Electronic Energy	9
Rotational Energy - Rigid Rotor	11
Vibrational Energy - Harmonic Oscillator	13
Morse Potential	14
Vibrational Energy - Anharmonic Oscillator	17
Optical Selection Rules	19
Summary	21
III. Fourier Transform Spectrometer	22
Theory of Operation	22

IV. Experimental Apparatus	25
Introduction	25
Bomen Fourier Transform Spectrometer	25
Absorption Cell	26
Data Analysis	26
V. Experimental Procedures	27
Experimental Procedure	27
Preparation of the Sample Cell	27
Collection of Data	28
Peak Picking	33
Calibration of the FTS	34
Assignment of the Spectrum	35
VI. RESULTS	37
Introduction	37
Mathematical Representation	37
Term Value Approach	38
Direct Approach	44
Global Least Squares Fit	49
Rotational Expansion	54
Vibrational Bandhead analysis	57
VII. Discussions and Recommendations for Future Work	61
Introduction	61
Discussion	61
Recommendations	65
Bibliography	67

Vita	68
-------------------	-----------

List of Figures

Figure

2.1 Potential energy curves of the X and B states of Bromine	9
2.2 Morse potential energy curve	15
2.3 Anharmonic oscillator potential energy curve	18
3.1 Basic Michelson Interferometer	22
5.1 Detector responsivity curve	31
5.2 Spectral data plot	32
5.3 Corrected spectral data plot	32
5.4 Enlarged spectral data plot	33
5.5 Spectral calibration plot for the FTS	35
6.1 Graph of term value residuals plotted against J'' for the $v' = 1$ to $v' = 13$ band	41
6.2 Graph of the global term value residuals plotted against J'' for the $v'' = 1$ to $v' = 13$ band	43
6.3 Energy level diagram of the fine structure of a rotation-vibration band	45
6.4 Differences in direct fit on a single band	47
6.5 Differences using the direct method on all bands and averaging the coefficients	48
6.6 Plot of the residuals of the $v''=1$ to $v'=13$ band when global fit rotational coefficients are used	53
7.1 Residuals of $v''=2$ to $v'=18$ band using Barrows constants	62
7.2 Plot of the residuals of the $v''=2$ to $v'=18$ vibrational band with best fit coefficients from this study	62

List of Tables

Table

1.1 Molecular constants for $^{79}\text{Br}_2$	5
6.1 Term value calculated values of B and D for the a single band fit and a global	40
6.2 Direct fit calculated values of B and D for a single band and an averaged fit.....	47
6.3 Summary of the Rotational constants (cm^{-1}) for the $X^1\Sigma_g^+$ state $^{79}\text{Br}_2$	52
6.4 Summary of the Rotational constants (cm^{-1}) for the $B^3\Pi(0_u^+)$ state of $^{79}\text{Br}_2$	52
6.5 Rotational Molecular constants (cm^{-1}) r the 79-79 isotope of diatomic bromine	57
6.6 Electronic and Vibrational constants (cm^{-1}) to fit the vibrational levels $v''=0-3$ with $v'=10-33$	58
6.7 Summary of vibrational Molecular constants (cm^{-1})	60

Abstract

High resolution Fourier Transform Absorption Spectroscopy has been conducted for the $B^3\Pi(0_u^+) \leftarrow X^1\Sigma_g^+$ system of $^{79}\text{Br}_2$. A total of 64 vibrational levels, including $v'' = 0-3$ and $v' = 10-33$, have been observed and assigned. Rotational levels as high as $J=76$ were observed. A global fitting routine has been developed to fit the rotational spectra to the Dunham Expansion. Using B_v and D_v for both the X and the B state, rotational transitions were calculated to within 0.02 cm^{-1} . The expansions of these terms required five coefficients for the B state and three coefficients for the X state. Attempts to fit the vibrational spectrum to an equation in terms of $(v+1/2)$ were only accurate to within 0.03 cm^{-1} when five molecular coefficients were used on the upper level and three were used on the ground state. However, direct calculation of the vibrational energy levels was able to fit all vibrational bandheads to less than 0.02 cm^{-1} . Recommendations are made for attempting a global fit over many more vibrational bands.

High Resolution Fourier Transform Absorption

Spectrum of $^{79}\text{Br}_2$ $B^3\Pi(0_u^+) \leftarrow X^1\Sigma_g^+$

1. Introduction

Overview

In recent years, much effort has been spent in the Air Force on the development of kilowatt-class lasers operating at infrared wavelengths in the anticipation they could be used for electro-optic countermeasures. One of the ways of transferring energy into the laser medium is through electronic to vibrational energy transfer mechanisms. A candidate system involves the photolysis of bromine. The present research seeks to extend the spectroscopic data base for the $B^3\Pi(0_u^+) \leftarrow X^1\Sigma_g^+$ electron transition of $^{79}\text{Br}_2$.

To do these studies most effectively, there must be a good base of knowledge about bromine from which to start. By far, the most extensive work to date on bromine is the high resolution work using grating instruments performed by Barrow, et al [1] and the complementary work performed by Coxon [3]. These studies yielded spectroscopic data over the range $0 \leq v'' \leq 10$ in the Br_2 $X^1\Sigma_g^+$ ground state and nearly all the bound vibrational levels of the Br_2 $B^3\Pi(0_u^+)$ excited state. The work done by Barrow in 1974 currently provides the best recorded set of spectroscopic constants available. This

thesis reports on Fourier Transform Spectroscopy performed to refine the molecular coefficients reported by Barrow. Data will be gathered and ways of analyzing this data will be developed.

Background

Bromine absorbs energy very readily in the visible to near IR wavelengths. The absorption continuum begins at 510.8 nm and thus we should expect to see strong transitions at wavelengths above this value [8]. At room temperature, spectrum should be readily obtainable up to about 625 nm. This is the rough value of where the long wavelength end of absorption out of the $v''=3$ level stops. Higher ground state levels than this will generally not have enough population in them to exhibit strong absorption characteristics for short absorption paths. The rotational energy level spacing is very small and will make the spectrum observed very dense in structure. The advent of today's digital processing technology makes this dense structure manageable. The peaks can be isolated and analyzed very readily.

Problem Statement

Recently, a large amount of work has been done at the Air Force Institute of Technology (AFIT) on the energy transfer kinetics of bromine. For these studies to be done effectively, the potential energy curves of bromine must be known. As the current best available comprehensive work done on this molecule was accomplished using grating instruments, it is the goal of this research to further, and hopefully improve, the

knowledge on the B and X states of bromine. This thesis effort consists of obtaining high resolution spectrum of $^{79}\text{Br}_2$ and developing the means to analyze it properly.

Summary of Current Knowledge

The first reported high resolution work done on $^{79}\text{Br}_2$ was accomplished by Horsley and Barrow [8]. This work consisted of identifying approximately 800 rotational lines of the spectrum between 510 and 610 nm. These lines were assigned to 10 different vibrational bands. From these observations, Horsley and Barrow were able to derive some of the rotational and vibrational constants. In their paper, they make no mention of how accurately they can reproduce the data. For this reason, and also for the fact that better coefficients are now available, the constants derived by Horsley and Barrow will not be reported.

Coxon [3] furthered the knowledge of the X and the B state by heating a sample of bromine and observing transitions on the long wavelength end of this system. This had the effect of significantly increasing the population in ground state vibrational levels with $v'' \geq 4$. In this study, the first accurate data for the vibrational levels $1 \leq v' \leq 9$ and $4 \leq v'' \leq 10$ was observed. Using these transitions, Coxon was able to come up with improved coefficients for the ground state.

With this prior knowledge as a starting point, Barrow, et al, was able to greatly increase the data available on the B-X system [1]. Using a high resolution grating instrument, they were able to catalog 88 bands of the $^{79}\text{Br}_2$ B-X system including levels

with $0 \leq v'' \leq 10$ and $1 \leq v' \leq 55$. Constants for the B state were determined both by direct fit and term value methods, but they were constrained to the values of B_v'' and D_v'' already determined by Coxon. Barrow discovered that the results of direct fitting methods are preferable to term value methods.

Using the data he acquired on the $^{79}\text{Br}_2$ B-X system, Barrow was unable to fit the data to a single Dunham expansion. The entire ground state could be fit effectively, but at high vibration levels in the B state, the G_v term could not be represented by simple polynomials. However, Barrow was able to derive constants for the B state that fit an arbitrarily chosen range of $v' \leq 8$. One of his observations was that double precision arithmetic would probably reduce the errors in his calculations.

To overcome the problem with being unable to fit the rotational and vibrational constants to simple polynomials, Barrow chose another method to report his data. He simply listed the values obtained for B_v , D_v and the vibration level origins directly. According to his study, all rotation transitions observed could be calculated to within 0.02 cm^{-1} . Barrow does not mention the range of J values that were observed. One extract from the paper indicates that the range on J probably only went out to about 50. The coefficients derived by Barrow can be seen in Table 1.1.

Scope

The objective of this thesis research will be to first obtain high resolution absorptio spectra of the $^{79}\text{Br}_2$ $\text{B}^3\Pi(0_v^+) \leftarrow \text{X}^1\Sigma_g^+$ system. A Bomen Fourier Transform

Table 1.1 Molecular Constants (cm^{-1}) for the X and B states of $^{79}\text{Br}_2$ [Barrow]

T_e	15902.47	
ω_e	167.60660	
$\omega_e x_e$	1.63608	
$\omega_e y_e$	-9.3687	
		B state
$10^2 B_e$	5.95890	
$10^4 \alpha_e$	4.89095	
$10^6 \gamma_e$	-6.63690	
$10^8 D_e$	3.01300	
ω_e	325.32130	
$\omega_e x_e$	1.07742	
$\omega_e y_e$	-2.29798	
		X state
$10^2 B_e$	8.21070	
$10^4 \alpha_e$	3.18730	
$10^6 \gamma_e$	-1.04500	
$10^8 D_e$	2.09200	

Spectrometer will be used to accomplish this task. Then, an attempt will be made to fit to fit this data to a single set of spectroscopic constants. The results of this effort will then be compared to the work of Barrow, and if necessary, the previous coefficients will be refined.

Summary

This completes the introductory portion of this thesis. Chapter II will describe the basic theory needed in describing the energy levels within a diatomic molecule with an explanation of the Dunham expansion. Chapter III is used to give a brief overview on Fourier Transform Spectroscopy since this is the way the data will be acquired. Chapters IV and V will concentrate on the experimental apparatus and procedures used to collect data. Chapter VI contains the results obtained in this research, while Chapter VII will present any conclusion, reached from this work as well as provides recommendations for future study.

II. Theory

Diatomic Molecules

A diatomic molecule is composed of two atoms. These atoms may or may not be of the same isotope (i.e. $^{79}\text{Br}^{81}\text{Br}$, $^{79}\text{Br}_2$, HCl). The nuclei of these two atoms are located within the electronic charge cloud which, when combined with the internuclear repulsion, gives a potential denoted by $V(r)$, where r is the internuclear separation [5]. This entire system is free to move about in three dimensional space, with six degrees of freedom (1 vibrational, 2 rotational, 3 translational). One useful way to break this energy into a usable form is to say that the energy of the electrons and the two nuclei are separable. In other words,

$$E_{tot} = E_{elec} + E_{nucl} \quad (2.1)$$

where E_{tot} is the total energy of the molecule, E_{elec} is the energy associated with a particular electronic state, and E_{nucl} is the energy associated with the nuclei. This equation can be rewritten as

$$E_{tot} = E_{elec} + E_{int} + E_{trans} \quad (2.2)$$

In this case, E_{int} is the internal (rotational, vibrational) energy of the molecule and is separable from E_{trans} , the energy associated with the translation of the molecule through free space.

Dunham Expansion

Now that we understand how the energy is partitioned, we need to find an equation for this energy that adequately represents the energy of any specific state the molecule might be in. For the case of the diatomic molecule, this energy can be adequately represented by an equation known as the Dunham expansion of the energy. This equation has the form

$$E = T_e + G_v + F_v(J) \quad (2.3)$$

where T_e is the energy associated with the electronic state of the molecule, G_v is the energy from its vibrational nature, and F_v is the energy associated with rotation. In particular,

$$G(v) = \omega_e(v + 1/2) - \omega_e x_e(v + 1/2)^2 + \omega_e y_e(v + 1/2)^3 + \dots \quad (2.4)$$

and

$$F_v(J) = B_v J(J+1) - D_v J^2(J+1)^2 + H_v J^3(J+1)^3 + \dots \quad (2.5)$$

where,

$$B_v = B_e - \alpha_e(v + 1/2) + \gamma_e(v + 1/2)^2 + \delta_e(v + 1/2)^3 + \dots \quad (2.6)$$

$$D_v = D_e - \beta_e(v + 1/2) + \eta_e(v + 1/2)^2 + \dots \quad (2.7)$$

$$H_v = H_e - \xi_e(v + 1/2) + \dots \quad (2.8)$$

The next several pages in this section will deal with the relevance of the terms in the Dunham expansion.

Electronic Energy

By far, the term with the largest amount of energy in the Dunham expansion is the electronic energy term. For bromine, this energy is on the order of 16000 cm^{-1} while vibrational energy is around 300 cm^{-1} . Fig. 2.1 is a graph of the potential energy curves associated with bromine. The value of T_e corresponds to the minimum of each potential well. The energy associated with vibration and rotation is additive above this point.

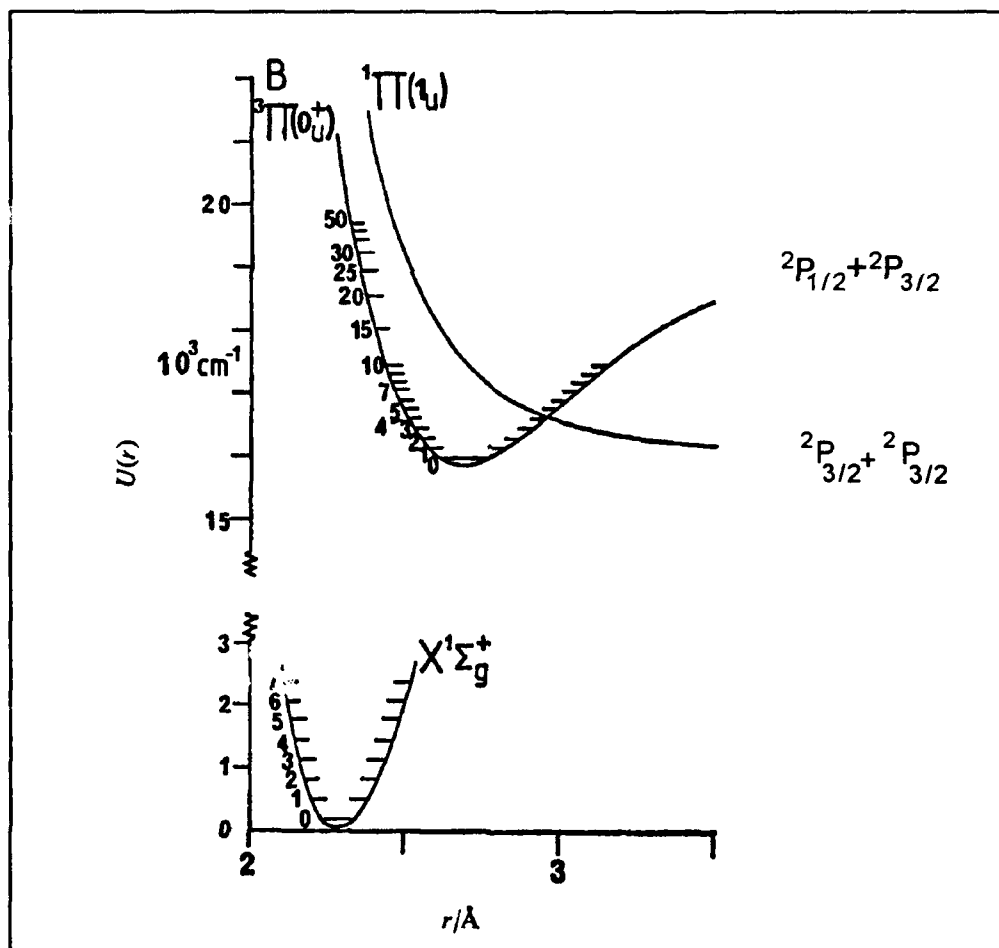


Figure 2.1 Potential energy curves of the X and B states of bromine

There are two separate extremes for a diatomic molecule in regards to internuclear separation. These extremes correspond to separations of infinity and near zero. The first case is most easily understood. Basically, there are two separate bromine atoms. Bromine belongs to the class of atoms known as the halogens. All these atoms have an outer electron shell with configuration p^5 . Accordingly, the first two atomic terms for these elements are $^2P_{1/2}$ and $^2P_{3/2}$. By Hund's rules, the $^2P_{3/2}$ term is the lower energy state, and in particular for the halogens, it corresponds to the ground state. A halogen designated by $^2P_{1/2}$ is in its first excited state. By looking at Fig. 2.1 (next page), we can see that if the X state curve were extended to dissociation, its product would be two ground state bromine atoms. Also, the state labeled $^1\Pi(1_u)$ would have the same dissociation products. However, the B state dissociates into one ground state and one excited state bromine atom.

The other extreme of the diatomic molecule is for very small internuclear separation. In this case, the wavefunctions of the two atoms overlap and they cannot be considered separately. Depending on the symmetry, the molecule will assume either a bound or repulsive posture. A bound state is one where there is a localized minimum of the potential energy curve. This shows that there is some point about which there can be oscillatory behavior. In Fig. 2.1, this situation exists for both the X and B states. The difference in these two states exists in the separated atom limit, where the symmetry properties of the B state will allow for one excited state atom while the X state will not.

Fig. 2.1 also shows another energy curve crossing through the B state. This state will produce two ground state atoms at its dissociation limit. It does not have a localized minimum and is known as a repulsive state. The behavior of a molecule in this state is very different than the oscillatory behavior of a bound state. There is a minimum distance for the internuclear separation. But once the molecule oscillates back away from this minimum, there is no maximum. Thus, the molecule will simply drift apart and dissociate. Probably the most interesting aspect of this state is that part of it is collocated (same energy for a particular separation) with the B state. This allows for interaction between the two states. It is possible for a molecule in the B state to transform its properties to those of the repulsive $^1\Pi(1_u)$ state. The mechanism for this transformation is unimportant. An initially bound molecule will now be in a repulsive state and head toward dissociation. The net result is to remove population from the B state through non-radiative means. This process happens at B state vibration levels greater than 5.

Rotational Energy - Rigid Rotor

The diatomic molecule has freedom to rotate about its center of mass. The energy associated with rotation along the axis joining the two molecules is negligible and can be ignored. The rotation through an axis perpendicular to this first axis is twofold degenerate and can be equated to the energy of a rigid rotator.

In the simplest form of this rotation, the diatomic molecule can be equated to a dumbbell. The two atoms can be considered to be point-like and connected to either

end of a weightless rigid rod. The effect of this first assumption is negligible as the mass of an atom is practically concentrated at its nucleus which has a diameter on the order of 10^{-12} , while internuclear separation is on the order of 10^{-8} [5]. The effect of the assumption of the rigid rod is small, but measurable. This will be accounted for later, but for now it is a good first approximation.

The kinetic energy associated with the rotation of this dumbbell is

$$\hat{H} = \frac{1}{2} I \omega^2 \quad (2.9)$$

where I is the moment of inertia and ω is angular velocity. This energy can be used to solve the Schrödinger equation in spherical coordinates. For the case of the rigid rotor, the potential energy term is zero. The final result of this equation is that the energy levels of the rotor are found to be

$$E = \left(\frac{\hbar^2}{2I} \right) J(J+1), \quad J = 0, 1, 2, \dots \quad (2.10)$$

where \hbar is Planck's constant and J is the rotational quantum number. The form of the equation above shows the energy of the rotor increases quadratically with J in discrete energy steps. More importantly, this term also has the same functional form of the first term in the rotational expansion part of the Dunham Equation (Eq 2.5). The coefficient above can be equated to

$$B_v = \frac{\hbar^2}{2I} \quad (2.11)$$

Vibrational Energy - Harmonic Oscillator

A first approximation of the vibrational energy of the diatomic molecule is to assume the molecule behaves as a nonrotating harmonic oscillator. In other words, the restoring force between the two atoms goes as

$$F = -kx \quad (2.12)$$

where k is the stretching force constant of the bond and x is the displacement of the system from equilibrium [5]. The potential energy related to this force is given by

$$\frac{dV(x)}{dx} = -F(x) = kx \quad (2.13)$$

Therefore

$$V(x) = \frac{1}{2} kx^2 \quad (2.14)$$

This potential energy can then be used in the Schrödinger equation to solve for the energy values of the system. This solution is

$$E(v) = (v + \frac{1}{2})h\nu_0 \quad (2.15)$$

where v is the vibrational quantum number and can assume integer values starting at zero. Again, it needs to be noted that the form of this equation is seen in the Dunham expansion. It corresponds to the first term in the vibrational energy expansion (Eq 2.4). The energy obtained by this treatment differs from the classical oscillator in two major forms. First, the energy is quantized. Second is the inclusion of the $1/2$ term. This

tells us that even for the lowest energy level, the energy is still not zero. This goes in keeping with the precepts of the uncertainty principle.

Morse Potential

These two approximations do not fully represent the energy of the molecule for several reasons. For starters, the rotational and vibrational energies are not separable. As a matter of fact, they are very much interrelated. The idea of a rigid rotor is in direct contradiction to the concept of an oscillator. Whereas the motion of the oscillator has an effect on the rotational motion, the rotation of the molecule has an effect on the vibration. But more importantly, the potential energy functions used are inappropriate. The harmonic oscillator potential does not allow for the molecule to dissociate at large internuclear separations. A more appropriate potential would allow for this dissociation.

The functional form on the potential must be modified. Figure 2.2 (next page) represents the $V(r)$ potential for a typical diatomic molecule. In this case, r is the internuclear separation of the two molecules. At large separations, the interactions between the two atoms is negligible, and the total energy is that of the two separated atoms. This energy can be arbitrarily taken to be the reference level $V(\infty) = 0$. As the two atoms are brought together from large separation, there is initially an attractive force between electrons on one atom and the nucleus on the other, and vice versa. This is the part of the curve below the reference line. If the atoms are brought still

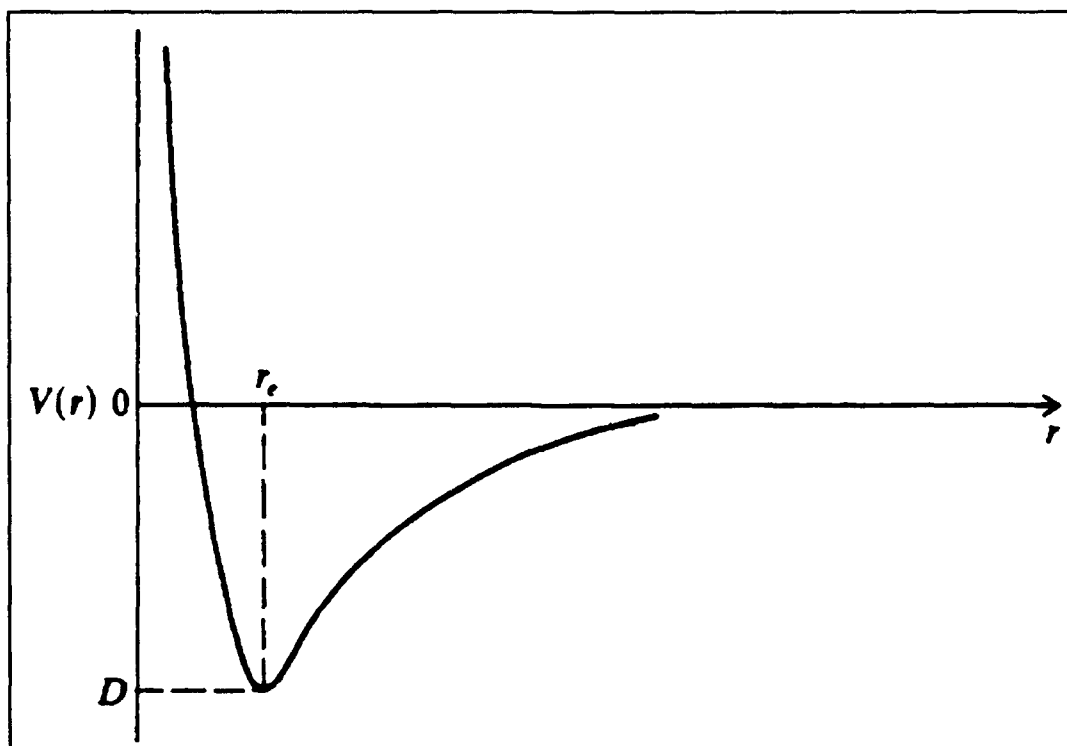


Figure 2.2 Typical potential function for a stable diatomic molecule [5:134]

closer together, the electron clouds begin to interpenetrate and the mutual repulsion starts to increase. Also, at these very small internuclear separations, nuclear-nuclear repulsion becomes important. It can also be seen that there is a minimum in the potential at some specific point in the curve. This point is known as the equilibrium point, r_e .

One way of modeling this potential analytically is with a functional form developed by P.M. Morse in 1932. Mathematically, this potential is represented by the equation

$$V(r) = D[1 - \exp(-a(r - r_e))]^2 \quad (2.16)$$

where a is a measure of the curvature of the function, and D is the depth of the

potential well. This is not the only function that will qualitatively describe the interactions of atoms in a diatomic molecule. There are other functional forms. But it does meet the minimum requirements. Namely, the potential has a minimum at r_e and its first derivative is zero at this point, it asymptotically approaches a constant value at infinity, and as $r \rightarrow 0$ the potential goes to infinity. This last condition is necessary because it describes the impossibility of the two nuclei being located on top of each other.

Before we can use this potential in the Schrödinger equation, we must first find the true equations of motion of the system. When we do this, a very interesting observation is made. Two of the three equations are identical to those arrived at in the rigid rotor approximation. Thus, we can assume there to be a form of the rigid rotor energy in the final solution. When this energy is coupled back into the radial equation, we get the following spherical equation of motion:

$$\frac{1}{r^2} \frac{d}{dr} r^2 \frac{dR}{dr} + \left\{ \frac{2\mu}{\hbar^2} [E - V(r)] - \frac{J(J+1)}{r^2} \right\} R = 0 \quad (2.17)$$

It is this equation that provides the true benefit of the Morse function. When it is substituted into the above equation, it allows for a direct solution of the vibrational part of the motion, and for a series solution to the rotational motion. This solution, to terms in second order in v and J , has the form [5:701]

$$E(v, J) = h[\omega_e(v + \frac{1}{2}) - \omega_e \chi_e(v + \frac{1}{2})^2 + B_e J(J+1) - D_e J^2(J+1)^2 - \alpha_e(v + \frac{1}{2})J(J+1)] \quad (2.18)$$

If the right side of Eq. 2.17 is divided by h , it very closely recreates the Dunham expansion mentioned earlier in this paper. The difference arises from the fact that the Dunham equations carries more perturbation terms on the vibrational energy. If terms to higher order in J had been carried, then the rotational energy would have matched exactly. Thus, we now need to come up with an explanation for the third, fourth and fifth terms in the above solution. We will skip the second term momentarily and explain it in the next section. The fourth term arises from the centrifugal stretching of the molecule and is proportional to J^4 . Thus, we can see that this distortion term is more pronounced for higher rotational levels. The final term links the average moment of inertia with the rotational energy.

Vibrational Energy - Anharmonic Oscillator

The corrections to the vibrational energy occur because the molecule does not behave like a harmonic oscillator. If this was the case, the potential would be characterized by the parabola in Fig. 2.3. This potential, and consequently the restoring force would increase indefinitely with increasing separation from the equilibrium position. Obviously, as was previously discussed in the development of the Morse potential, this is not the case. The true potential is represented by the solid line curve in Fig. 2.3. At small displacements from equilibrium, this curve can be represented very closely by a parabola. This is why the harmonic oscillator model works so very well for small vibrations of the molecule [6].

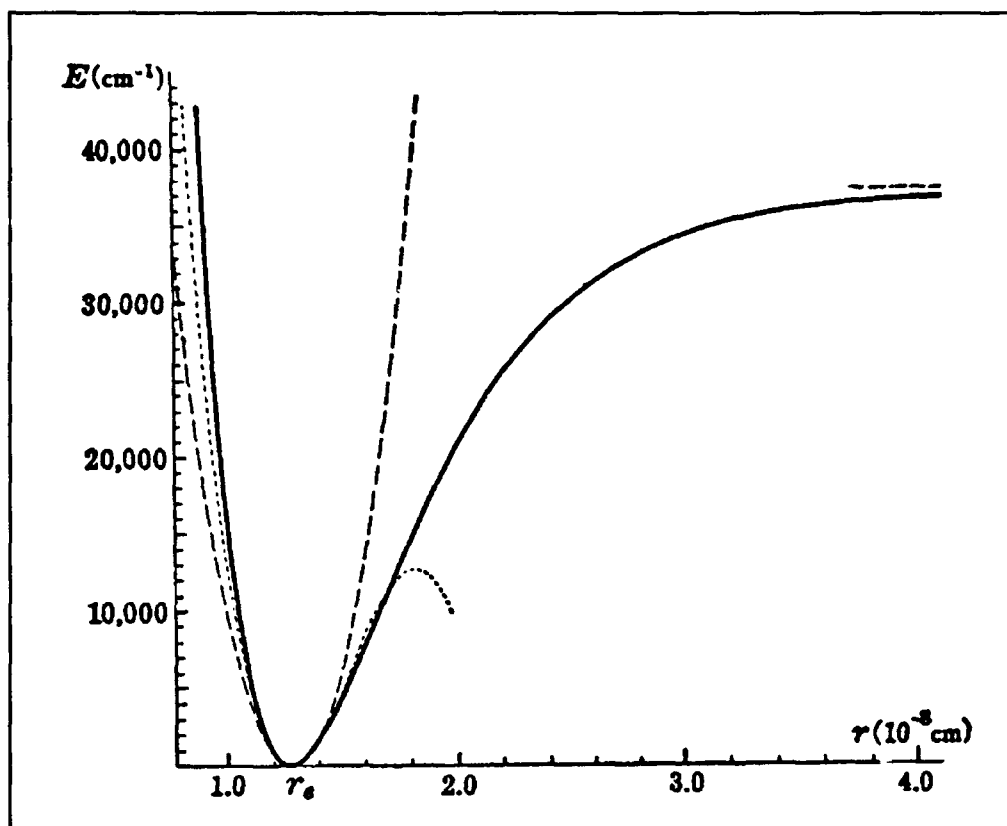


Figure 2.3 Comparison of typical ground state potential function with ordinary and cubic parabola approximations [6:91]

One of the easiest ways to make a first approximation to this potential curve is to add higher order terms to the form of the potential for the oscillator. For example, let

$$V(x) = \frac{1}{2}kx^2 - gx^3 + \dots \quad (2.19)$$

For this situation, the coefficient on the cubic term is much smaller than the coefficient on the quadratic term. This approximation can be seen by the dotted line in Fig. 2.3. Granted, this approximation does not match the whole of the actual potential energy curve, but it is a much better representation for small values of displacement. If terms to the fourth power and higher are added, the fit even more accurately represents the oscillator is now known as an anharmonic oscillator. The potential described by

[Eq. 2.18] gives the following eigen values when it is used in the wave equation

$$E_v = hc\omega_e(v + 1/2) - hc\omega_e x_e(v + 1/2)^2 + hc\omega_e y_e(v + 1/2)^3 + \dots \quad (2.20)$$

or, the term values are given by

$$G(v) = \omega_e(v + 1/2) - \omega_e x_e(v + 1/2)^2 + \omega_e y_e(v + 1/2)^3 + \dots \quad (2.21)$$

where v is the vibrational quantum number. For this solution, the coefficient on the first term is much larger than that on the quadratic term, which is much larger than that on the cubic term. For the form of the potential given in [Eq. 2.18], when g is positive, $\omega_e x_e$ is positive.

Eq 2.20 Tells something very interesting about the vibrational energy spacing in an anharmonic oscillator. Due to the quadratic and higher terms in the energy equation, the energy levels are no longer equally separated as they are in the case of a harmonic oscillator. Their separation decreases slowly with increasing v . The size of the quadratic coefficient in the energy equation helps determine how rapidly this decrease takes place. In that light, the $\omega_e x_e$ term gives a rough value for the degree of anharmonicity of the diatomic molecule. It also tells us how rapidly the molecule is prone to dissociation.

Optical Selection Rules

Now that the energy levels within a diatomic molecule have been represented mathematically, it is time to take a quick look at the energy transitions that will be

observed in this experiment. The transitions of interest are those between the X and the B state. Due to the position of these two energy curves (see Fig. 2.1), these transitions will correspond to photons in the $10000 - 20000 \text{ cm}^{-1}$ range.

As far as the vibration terms go, there are no restrictions on the change that can take place with the vibrational quantum number. Thus, ν can assume any number within its range for the electronic state it is in.

This is not the case for the change in the rotational quantum number, J . Here we have a requirement that the change in J must be ± 1 . Thus, there are only two transitions that can take place for each rotational energy level for any specific vibrational level.

For ease in keeping track of these transitions, a set of terminology has been set up to help keep track of the energy levels we are dealing with, as well as being able to more effectively track the rotational transitions. The first bit of terminology the use of prime and double prime notation. A quantum number with a prime on it (ν') is a quantum number associated with the higher energy level of the two states involved in a transition. A double prime (ν'') indicates the lower energy state. For the purposes of this experiment a single prime indicates the B state, while double prime is the ground state.

As mentioned earlier, the value of J can only change by ± 1 . Thus, transitions out

of a specific J'' must go to an upper level where $J' = J'' + 1$, or $J'' - 1$. When the transition is to $J'' + 1$, this is known as an R branch transition. Mathematically, the energy difference of this transition can be represented by the equation

$$R(J) = \nu_0 + B_v' J'(J'+1) - D_v' J'^2 (J'+1)^2 - [B_v'' J''(J''+1) - D_v'' J''^2 (J''+1)^2] \quad (2.22)$$

where ν_0 is the location of the vibration band origin and contains all the information about the difference between the respective T_0 and G_v terms. By making the substitution $J' = J'' + 1$, this equation becomes

$$R(J') = \nu_0 + B_v' (J'+1)(J'+2) - D_v' (J'+1)^2 (J'+2)^2 - [B_v'' J''(J''+1) - D_v'' J''^2 (J''+1)^2] \quad (2.23)$$

By using these same procedures, the P branch can be represented by the equation

$$P(J'') = \nu_0 + B_v' J''(J''-1) - D_v' J''^2 (J''-1)^2 - [B_v'' J''(J''+1) - D_v'' J''^2 (J''+1)^2] \quad (2.24)$$

Summary

Thus, in this chapter, we have accounted for all the terms in the Dunham expansion. We have also shown how to use the energy levels predicted by this model to come up with two series of rotational lines for each vibrational band. Finally, we have described some of the terminology to be used in spectroscopy.

III. Fourier Transform Spectrometer

Theory of Operation

The main data gathering tool in this research effort was a Bomen DA-8 Fourier Transform Spectrometer (FTS). Fig. 3.1 is a schematic diagram of the basic Michelson interferometer. This is the design utilized by the Bomen DA-8.

The best place to start is with the light source. A source is chosen so as to match the spectral region of interest. Glowbars are a good source for the near infrared, while quartz lamps work well in the visible regions [2]. The light from the source is collimated

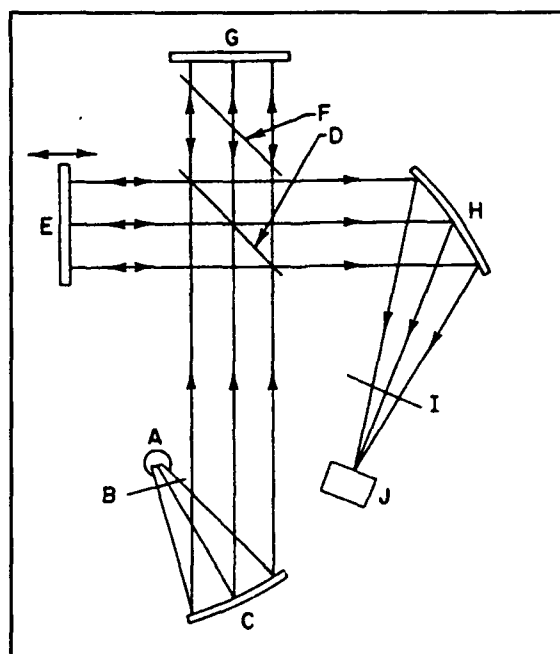


Figure 3.1 Basic Michelson interferometer. A: source. B: chopper. C: Collimator D: Beamsplitter. E: Movable Mirror. F: Compensator. G: Fixed Mirror H: Focusing Mirror I: Spectral Filters. J: Detector. [2:18]

and passed to a beamsplitter where it is amplitude divided. One part of the beam is passed through a compensator plate and then reflected off a fixed mirror. From here, it is passed back through the plate, reflected off the beam splitter and passed to a focusing mirror. The other part of the beam is reflected off the beamsplitter and towards a mirror on a translatable mount. This mirror reflects the light so that it passes back through the beamsplitter and onto the focusing mirror. The purpose of the compensator plate is to help keep the optical paths of the two arms at approximately the same length. This is necessary because the majority of the radiation reflected to the movable mirror comes from the second surface of the beamsplitter the light encounters, not the first. The role of the focusing mirror is to pass the recombined light to an intensity sensitive detector.

Varying degrees of spectral interference are created by an optical path difference in the two arms of the interferometer. Since the light must travel to and from each of the mirrors at the end of the arms, the optical path difference is equal to two times the mirror displacement from the neutral position. This optical path difference can be to either side of the neutral position, as the interference pattern is the same in both directions.

Each wavelength of light produces its own unique interference pattern as the position of the movable mirror is varied. If the light source was monochromatic, the signal seen by the detector would be a simple sinusoid as a function of mirror position. The frequency of this sine wave would be unique to the wavelength. Since a broad

spectrum light source is used in the FTS, there are virtually an infinite number of wavelengths of light that are all exhibiting the above mentioned behavior. When these different wavelengths are combined back at the focusing mirror and sent to the detector, they create an interference pattern. This pattern, the sum of the fluxes of each individual wavelength from the light source, is called an interferogram. Fourier analysis of this pattern allows the interferogram to be broken into its components. Each component corresponds to a different wavelength [2]. So, now all the wavelengths reaching the detector are known so long as they fall within the dynamic range of the detector.

For the purpose of this experiment, after the light is recombined and before it is passed to the detector, it is first passed through an absorption cell containing the bromine. Photons with the proper energy to cause a transition from one energy level to the next are absorbed and the rest are allowed to pass through. Thus, the interferogram is now modified from what it looked like originally. The intensity at some wavelengths has been reduced. When the Fourier transform of this modified interferogram is taken, the previous broad spectrum of the light will now have minimums where photons have been absorbed. These account for the reduced number of photons of these energies reaching the detector. When this spectrum is inverted, these minimums become maximums, and they correspond to the energy transitions of interest.

IV. Experimental Apparatus

Introduction

This chapter describes the experimental apparatus used in this research effort. The major subsystems include the Bomen Fourier Transform Spectrometer, the absorption cell and a 486-DX50 personal computer.

Bomen Fourier Transform Spectrometer

A Bomen DA-8 Fourier Transform Spectrometer (FTS) was used for data collection. This FTS has 50 cm of translation available on its upper mirror and allows for resolutions as small as 0.02 cm^{-1} . The absorption cell is placed internal to the FTS in a built in sample chamber. A quartz lamp is used for illumination due to its broad spectrum in the visible wavelengths. This beam is passed through a quartz beam splitter, recombined, shined through the absorption cell and then directed into a Cincinnati Electronics silicone avalanche detector. This detector has an operating range of $9000\text{-}22000\text{ cm}^{-1}$. A combination of long pass and a short pass filters are placed between the port where the light enters the sample chamber and the silicone detector. This effectively acts as a band pass filter for the input to the detector.

Absorption Cell

The absorption cell is a 35 cm long Pyrex tube that is 5 cm in diameter. An Oriel #45603 two inch glass window is placed on both ends of the tube. This window was picked due to its high transmission in the 350-800 nm range. There are three outlet ports on the glass tube. Two of them have valves fitted in them and the third is a straight glass tube. This design allows the cell to be used either as a straight absorption cell (as in this experiment), or would allow metered amounts of a substance to be admitted while still having a port available for either pressure or temperature measurements. The absorption cell was filled 90% atm enriched $^{79}\text{Br}_2$ that was obtained from Icon.

Data Analysis

A Beta version of Bomen's PC-D8 software was used to run the FTS. The most important attributes this software allows the user to select on the FTS are the wavelength region of interest, the resolution desired, and the number of scans on the FTS. Furthermore, once the FTS was finished acquiring data from a particular run, this software was able to calculate the Fourier transform of the signal received. This information was then stored in a file to be accessed by GRAMS 386, a data analysis package from Galactic Industries Corporation.

V. Experimental Procedures

Experimental Procedure

The purpose of this section is to explain the methods used to collect data for this experiment.

Preparation of the Sample Cell

As mentioned earlier, the absorption cell was a 35 cm long Pyrex tube with glass windows on either end. These windows were attached to the tube with Torr Seal. This product was preferred over the other epoxies available in the lab because it appeared to be the only epoxy not to be absorbing the bromine. Once the windows were attached to the tube, the epoxy was allowed to dry overnight and then the cell was attached to a vacuum. The absorption cell was evacuated to less than 3 mTorr, and the vacuum pump was left to pull on the cell for approximately seventy-two hours. The purpose here was twofold. The first was to see whether or not a good seal was actually present on the cell. The second was to help speed up the outgassing process of both the cell and the epoxy.

Once the outgassing of the epoxy was finished, the leak rate of the cell was checked. The leak rate was found to be less than 0.5 mTorr/minute. This was deemed an acceptable rate so as not to create significant pressure broadening of the spectrum once bromine was put in the cell.

In order to put the bromine into the cell, the cell was connected to a vacuum system on one of its valve ports and to a source of isotropically enriched bromine on the other. The vacuum was turned on, and the internal pressure of the cell was pulled down to approximately 3 mTorr. The valve to the vacuum was then closed, and the valve to the bromine was opened. The system was allowed to come to equilibrium, and then the valves to both the absorption cell and the bromine source were closed. This process allowed 60 Torr (vapor pressure) of bromine to be admitted to the absorption cell. This high vapor pressure of bromine is why the small leak rate on the cell was deemed to be insignificant to causing pressure broadening.

Collection of Data

The same process was used to collect all the data in this experiment. It will only be explained once here. The only difference in the data runs were the number of scans that were made on the FTS, the resolution that was selected, and the filters that were placed in the sample chamber.

There were several bits of data that had to be input to the FTS prior to each data run. The first was the number of scans of the mirror. There is no hard and fast rule for this decision. One must perform enough scans to get valid data from the area of interest, but this must be weighed with the amount of time necessary to complete the scans. For the purposes of this experiment, all data runs were accomplished with 128 scans of the mirror, while all background runs were done with 64.

The next important piece of data to input was the resolution desired from the data run. This number was variable from 4.0 cm^{-1} to 0.02 cm^{-1} . Low resolution runs to locate the bandheads were done at 2.0 cm^{-1} resolution while high resolution runs to find the rotational transitions were done at 0.02 cm^{-1} . The background samples for the high resolution runs were accomplished at 1.0 cm^{-1} . This number for background resolution was selected because an analysis of one of the background runs revealed there was no repeatable structure present in its spectrogram. The purpose of the background run was merely to smooth out the artifacts of numerical filtering and variable detector response of the actual data runs (more on this later).

The last parameter to be set on the FTS was the wavelength region of interest. Ideally, the whole wavelength region could have been calculated for each data run. Due to the limits of the processor in the FTS, this was not always possible. For resolution runs above 2.0 cm^{-1} , the entire region of interest from 13500 to 20000 cm^{-1} could be calculated on one data run. However, at resolutions smaller than this, it was no longer possible. For example, when the FTS was put to its maximum resolution of 0.02 cm^{-1} , the largest piece of spectrum that could be calculated was 325 cm^{-1} wide. It needs to be pointed out that this was a numerical constraint and not a physical one. The whole wavelength region was still passing into the detector and an interferogram of the whole region was still present. The processor was merely incapable of calculating a larger area at this resolution.

This leads to the next consideration. As mentioned earlier, a combination of long and short pass filters were placed in the sample chamber. The purpose here was to help improve the detector efficiency. If there was only a limited area of interest in the spectrum for each data run, it made no sense to have unwanted photons impinging on the detector. These photons would merely degrade the detector's operation without adding anything to spectrum being analyzed. To minimize this problem, filters were selected so as to bracket the region of interest. For example, if the area analyzed was from 17050 cm^{-1} (587 nm) to 17350 cm^{-1} (576 nm), a 550 nm long pass filter and a 600 nm short pass filter were put into the chamber. This had the benefit of greatly improving the signal over the selected area of interest.

Data was now collected on the FTS. Runs at 2.0 cm^{-1} resolution could be collected in approximately 2 minutes, while a 128 scan run at 0.02 cm^{-1} required just under 8 hours. Immediately after each data run was completed, a background run was accomplished. This was done with the filters in the exact same position as for the data run. The purpose here was to ensure no error was being introduced by moving the filters. Also, the light beam was passed through two windows identical to the windows on the absorption cell. Again, this was to simulate the light path as closely as possible to the absorption cell with no gas in it. A background run required approximately 6 minutes when done at 1.0 cm^{-1} resolution and 64 scans.

As can be seen in Fig. 5.1, the response of the detector is not constant over the region of interest. As a matter of fact, it is not even linear. For this reason, it was

necessary to correct the spectrum for this responsivity. This was the purpose of the background run. Since the background run was taken so as to replicate the absorption cell with no bromine present, it can be assumed that the deviation of the spectrum during a data run from the corresponding spectra of a background run was due strictly

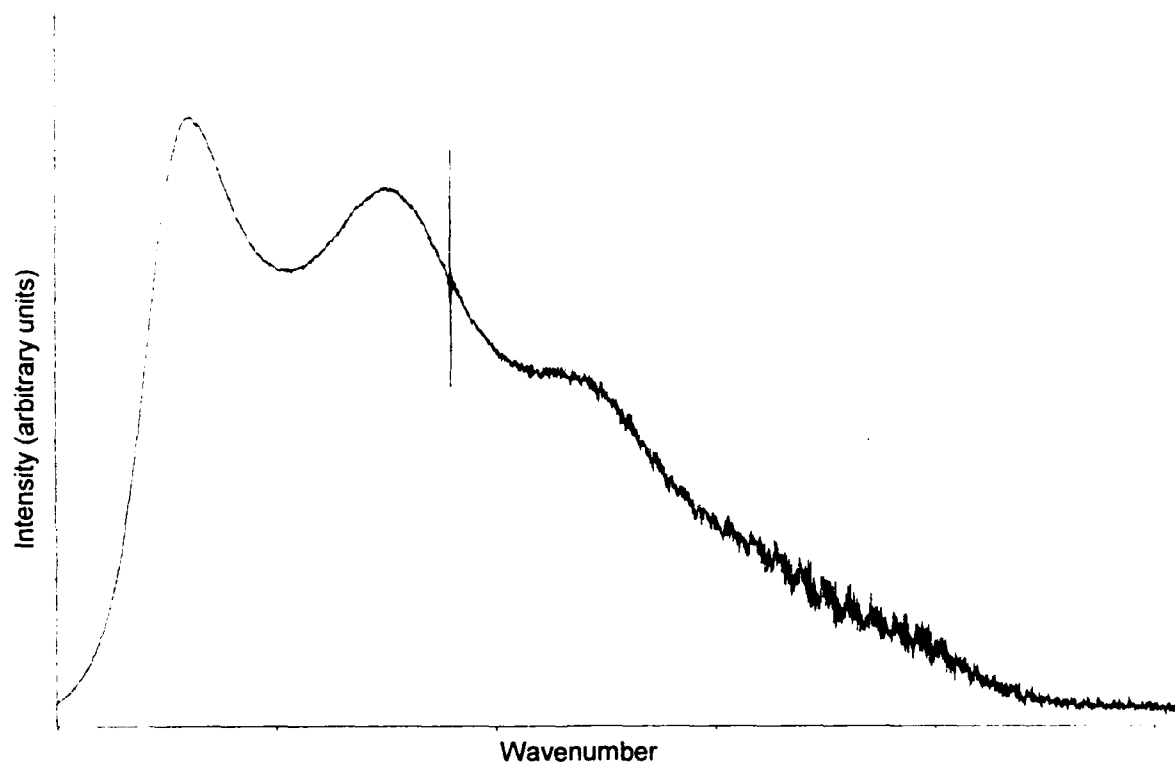


Figure 5.1 Graph of the detector response over the spectral range (cm^{-1}) of interest. The large spike in the graph comes from the HeNe laser used in calibration of the FTS.

to the presence of bromine in the cell. A sample of an uncorrected bromine data run can be seen in Fig. 5.2 (next page). This sample looks like Fig. 5.3 (next page) when the background correction was applied. There is a function built into the GRAMS software that automatically scales the data within a single run to the correct proportions. These spectrums were obtained from GRAMS 386. This program will take the Fourier transform calculated by the FTS and plot it out as function of wavelength

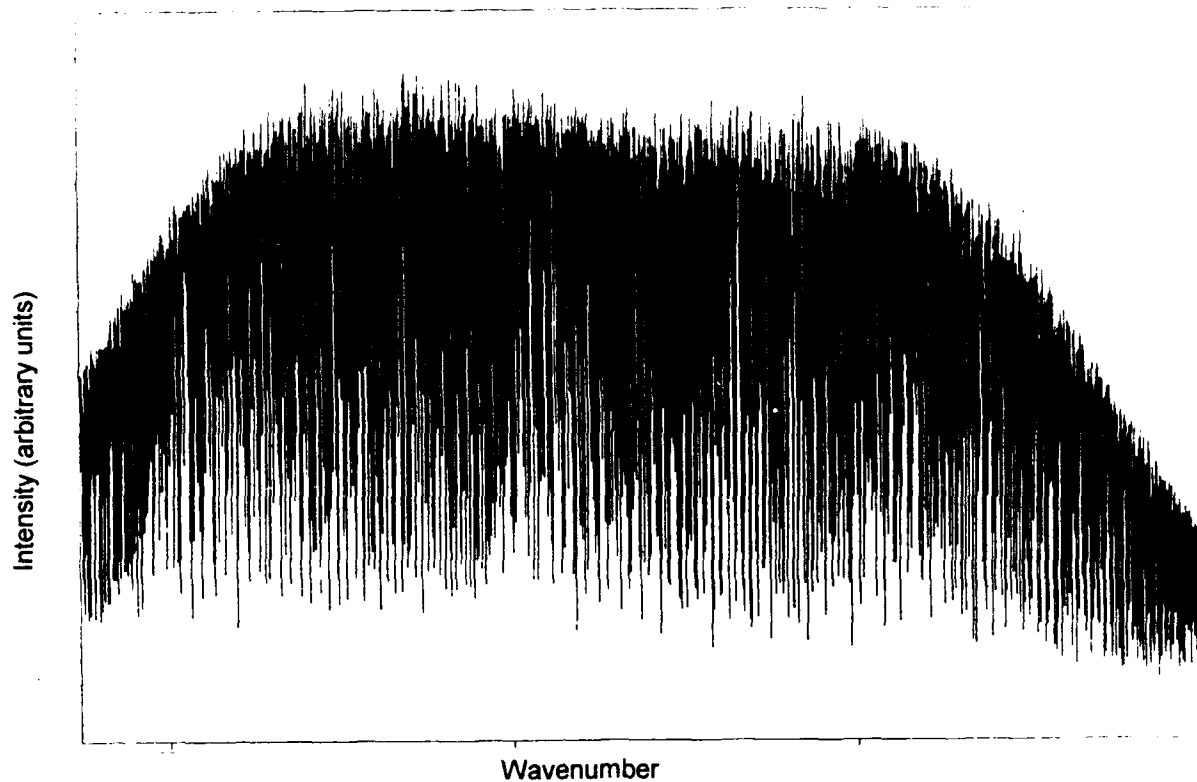


Figure 5.2 *Graph of data run with no background correction*

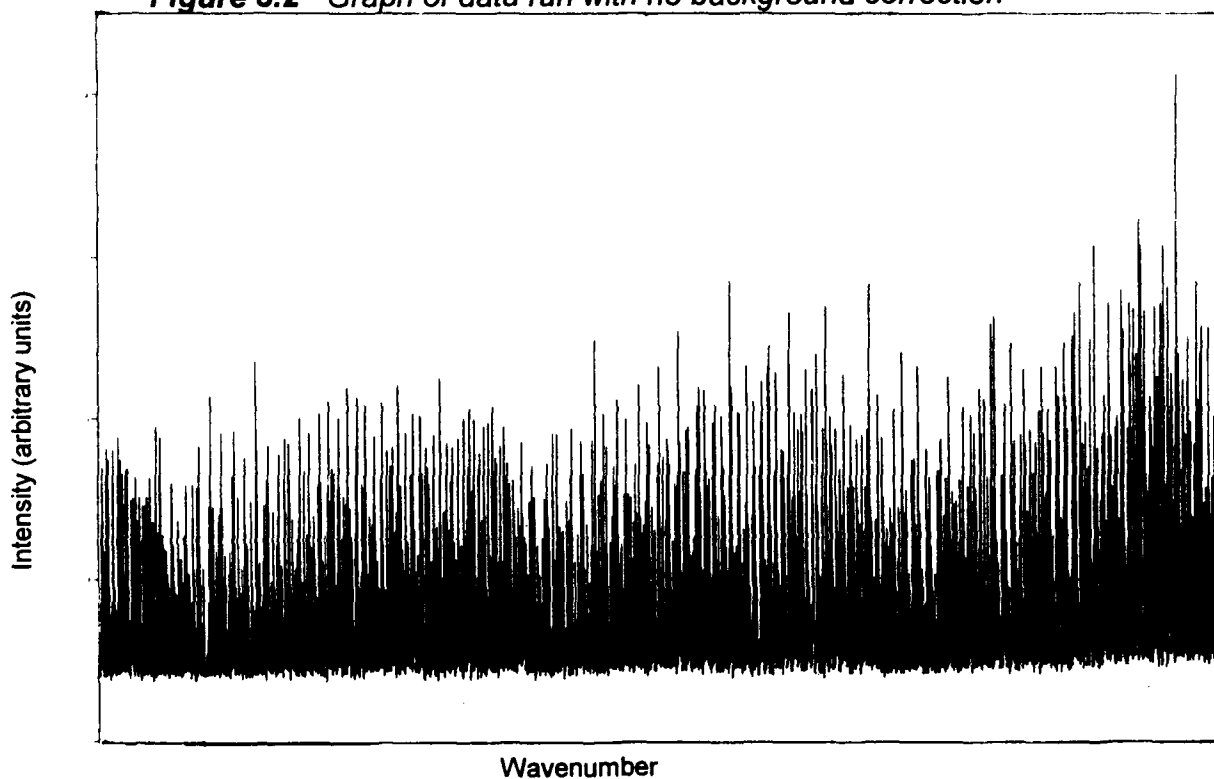


Figure 5.3 *Trace showing same data from Fig. 5.2 with background correction*

intensity.

Peak Picking

As can be easily seen in Fig. 5.3, the spectrum of bromine is very dense. As a matter of fact, at this stage it is hard to tell whether or not this is actually spectrum or just noise. Fig. 5.4 helps provide the answer to this question. This figure is a 25 cm^{-1} piece of the spectrum from Fig. 5.3. In this figure, the beginnings of periodic structure are just beginning to become discernible.

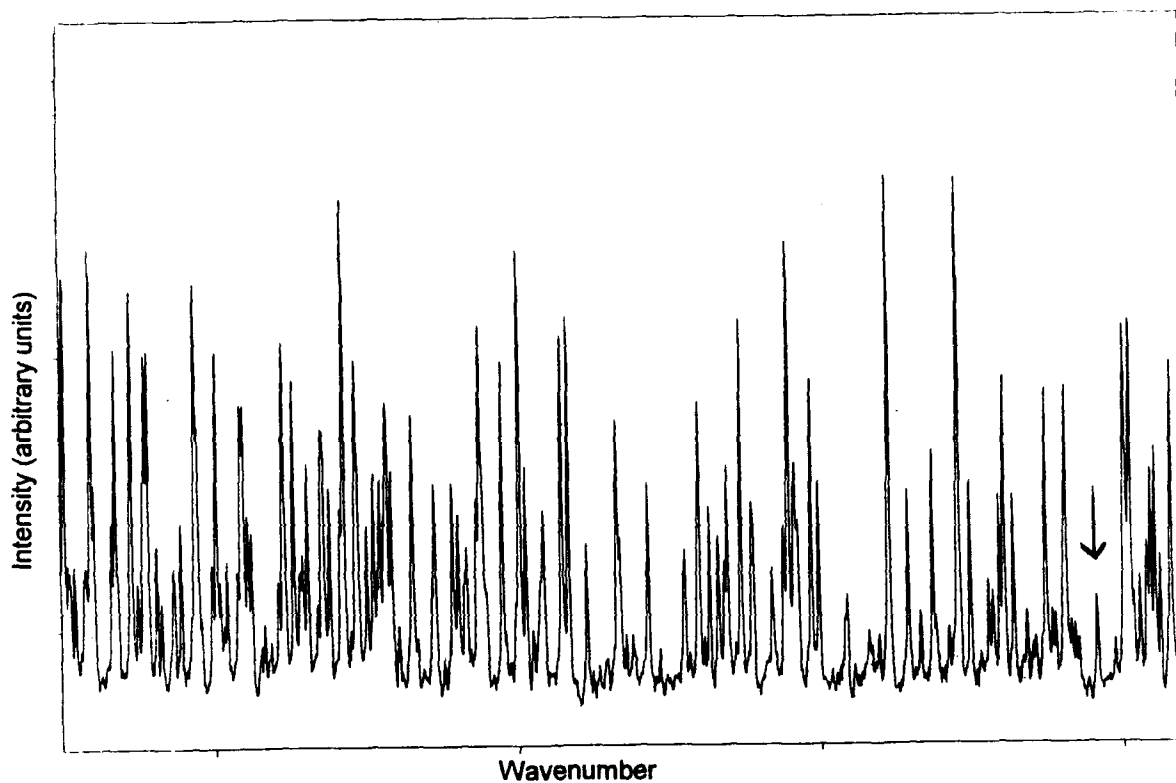


Figure 5.4 25 cm^{-1} wide piece of raw data that shows beginnings of rotational structure

Peak picking and the wavenumber assignment were accomplished using GRAMS 386. One of the less intense structures within the given spectrum that still appeared to

represent a rotational transition was first isolated on the computer screen. An example of a representative structure is indicated by the arrow in the Fig 5.4. This peak was designated as the baseline from which GRAMS would automatically select all the remaining transitions within the spectrum currently displayed. The benefit here was that only one peak needed to be designated manually, while all the remaining peaks on that data run were found by the computer. Considering there were usually over 1500 peaks in any given 300 cm^{-1} chunk, this was an enormous benefit. The wavelengths of all these peaks were then exported to a text file which was downloaded from the computer.

Calibration of the FTS

In order to determine if the FTS was calculating accurate values for the transitions, an iodine cell was used to calibrate the system. This cell was scanned at 0.02 cm^{-1} resolution over the range 16400 to 19300 cm^{-1} . The transitions observed on these scans were then compared to known spectroscopic data on iodine [4]. Fig. 5.5 shows a plot of the observed wavenumber of the transition versus the difference in its actual value. As can be easily seen, there is a systematic deviation of observed values versus actual values. A linear regression drawn through this data shows the majority of the points to be located within 0.01 cm^{-1} of the line. Due to this, a linear correction to the data was deemed an appropriate solution to the problem.

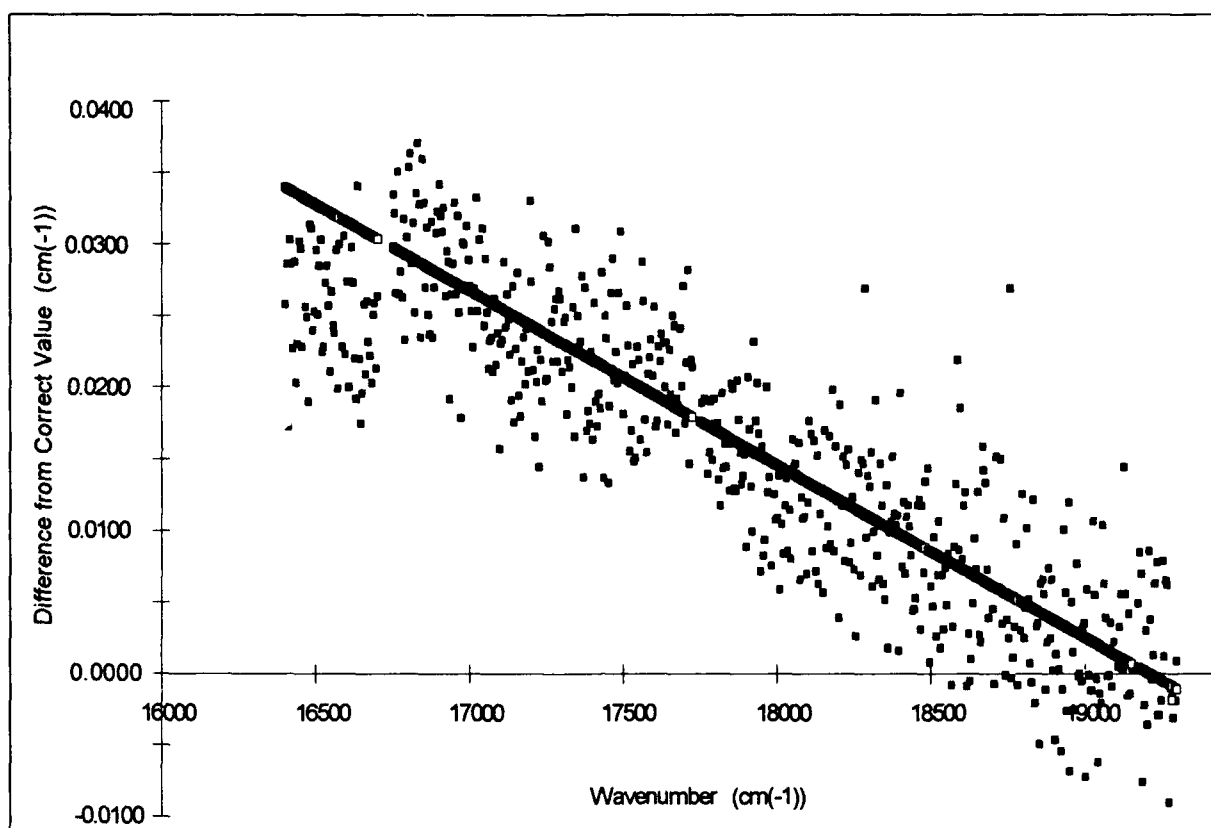


Figure 5.5 Calibration plot for the FTS

Assignment of the Spectrum

The basic premise for assigning the spectrum was that the work done by Barrow, et al, was correct. Using this as a starting point, the assignment of the rotational transitions was tedious, but straightforward. The alternation in the intensities of the transitions helped to distinguish one band from the next. This occurred when there were overlapping transitions from two different bands. By having a general idea as to

the intensity of the transition, it was possible to discard a peak as belonging to another vibrational band even when the wavelength of the transition corresponded to what was predicted.

The major deviation that was seen from Barrow's work was in the high rotational numbers ($J > 50$). In all bands observed, there was a systematic trend for these rotational transitions to occur at progressively longer and longer wavelengths. The magnitude of greatest deviation in each band varied from 0.03 to 0.20 cm^{-1} . The cause for this will be discussed in Chapter VII.

VI. RESULTS

Introduction

This chapter presents the results obtained in this experimental effort. The ultimate goal is a set of molecular constants that fully quantify the data. Three different methods of obtaining the constants from the data will be discussed. The *prima facie* method (Term Value approach) that appears to provide a global fit will be examined first. It will be shown why this is an inferior method to using a method of direct fit to each vibrational band. Then, a global least squares fit to all the rotational lines will be used to obtain the rotational constants. Finally, a fit will be attempted on the vibrational terms.

Mathematical Representation

As pointed out in the theory section, the rotational energy is represented by the equation

$$F_v = B_v J(J+1) - D_v J^2(J+1)^2 + H_v J^3(J+1)^3 + \dots \quad (6.1)$$

As this is an infinite series, the question must be asked as to how many terms need to be carried to adequately represent the data. This is an important question as the values obtained for B_v and, more particularly, for D_v , will depend on the model used. The goal of this research is to mathematically represent the data to within the resolution of the instrumentation used. Only as many terms as are necessary to achieve this goal will be included.

Term Value Approach

This approach gets its name from the method it employs. A set of terms are first calculated from the actual data. These terms are then used to find the rotational coefficients. The procedure for this is outlined in the following paragraphs.

This method uses the concept of differences between selected rotational transitions. As can be recalled from earlier in this paper, there are two different sets of rotational transitions that take place between two vibrational levels. These are the R and P branches. By taking the correct differences between these two branches, either the upper or lower state coefficients can be isolated. This works as follows. First, recall that an R branch transition is defined by the equation

$$R(J') = \nu_0 + B_v'(J'+1)(J'+2) - D_v'(J'+1)^2(J'+2)^2 - [B_v'' J'(J'+1) - D_v'' J'^2(J'+1)^2] \quad (6.2)$$

while a P branch is defined by

$$P(J') = \nu_0 + B_v' J'(J-1) - D_v' J'^2(J-1)^2 - [B_v'' J'(J'+1) - D_v'' J'^2(J'+1)^2] \quad (6.3)$$

Again, J'' is the rotational quantum number on the lower state. These equations assume a two term expansion sufficiently represents the data. They define the energy, or in effect tell us the wavenumber, associated with the appropriate transition. If one were to take a difference between the proper rotational transitions, an expression for either the upper or lower state constants is achieved.

For example, one difference that is of benefit is

$$R(J) - P(J) = 2B_v' - 4D_v' + (4B_v' - 12D_v')J - 12D_v'J^2 - 8D_v'J^3 \quad (6.4)$$

where J is the rotational quantum number of the lower level. The double prime convention on J will be dropped for the remainder of this paper for the purpose of ease in viewing the equations. All J 's will correspond to the lower state unless stated otherwise. As can be seen in Eq. 6.4, this difference is defined only in terms of constants of the upper vibrational state. The lower state constants have been removed. Similarly, another difference can be taken so there is an equation only in terms of the constants of the lower level. This difference is

$$R(J - 1) - P(J + 1) = 2B_v'' - 4D_v'' + (4B_v'' - 12D_v'')J - 12D_v''J^2 - 8D_v''J^3 \quad (6.5)$$

As mentioned earlier in this paper, there were 120-150 rotational transitions seen for each vibrational band. Generally speaking, half of these were P branch and the other half were R branch. Thus, there were 60-75 differences that could have been substituted into each one of the previous two equations for any particular vibrational band. To solve for the constants, we merely have to find the best fit to our over determined system. The method employed was to find the least squares fit to the system of equations at hand. This was accomplished using both Tablecurve and Mathematica. If this fit was done for both Eq. 6.4 and Eq. 6.5 using the transitions within one vibrational band, a single set of constants could be found to describe the upper and lower states of that particular band. For example, if the rotational

transitions associated with $v'' = 1$ to $v' = 13$ are used in this analysis, values will be obtained for B_v and D_v for both these vibrational levels. These values are seen in Table 6.1 As this fit is done on a single vibrational transition, we would expect there to be a good correlation between the observed and the calculated values for rotational

Table 6.1 Table showing the term value calculated values of B and D for both a single band fit and a global fit

	$10^2 B_v (cm^{-1})$		$10^8 D_v (cm^{-1})$	
	Single Band	Global	Single Band	Global
$v = 13$	5.1607	5.1621	4.8904	5.1347
$v' = 1$	8.1587	8.1623	1.6888	2.0755
	std dev < 0.0020		std dev < 0.40	

transitions within that band. Indeed, this is the case for the single band fit. An example of this correlation is demonstrated by Fig. 6.1 which is a graph of the difference between the observed and the calculated values as a function of the lower rotational quantum number for the rotational transitions within the $v''=1$ to $v'=13$ band. The significance of this graph is that the closer the points are to zero, the more accurately the mathematical model is representing the data. Granted, this graph is shifted off of zero, but this is easily explainable. Barrow's value for the vibrational bandhead has been used for the calculations. This is because the term value method does not provide this information. All values relating to T_0 and G_v have been removed in the difference equations. However, one can tell by looking at the graph of the differences, that there is relatively no trend for the data to move any farther away from zero than it already is. The fact that the zero reference line is not going through the data tells us

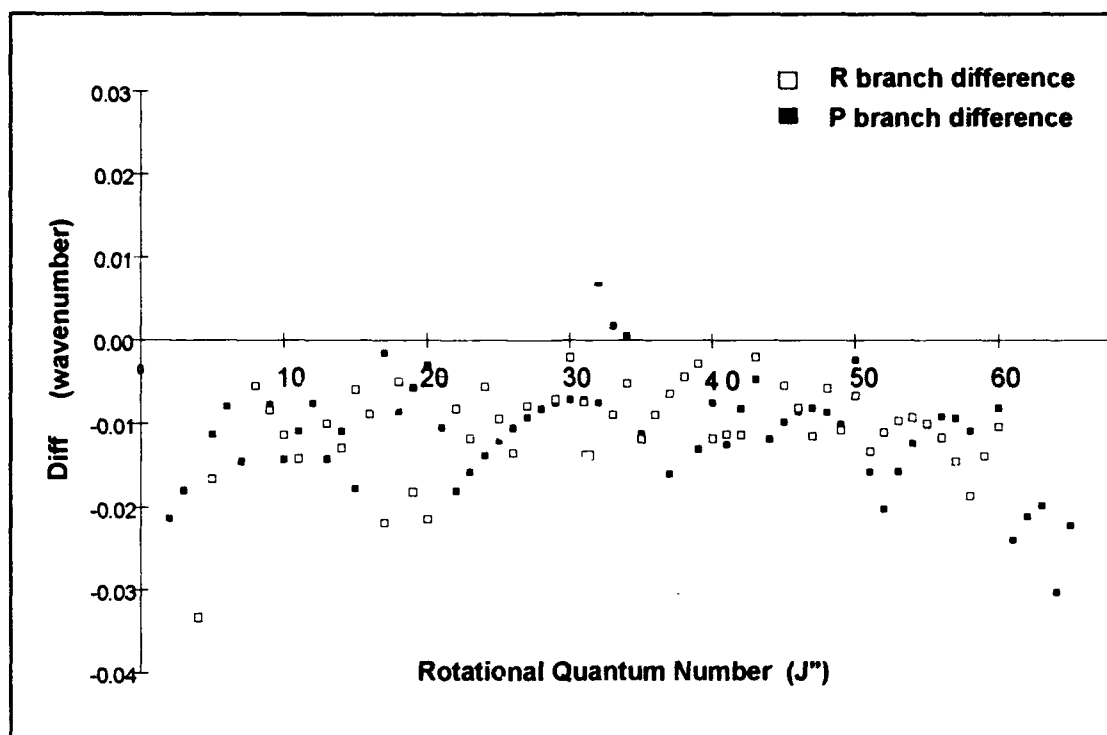


Figure 6.1 Graph of difference in observed value for rotational transition from calculated term value $[v(\text{observed}) - v(\text{calc})]$ for single band fit plotted against lower state rotational quantum number J'' for $v'' = 1$ to $v' = 13$ band

the assumption about the location of the vibration levels is in error. Thus, in this analysis of the rotational transitions, we have found out some information about the vibrational energies.

Now, back to the subject of the term value approach. As the last graph showed, it is possible to obtain a very accurate description of rotational constants for a single vibrational band. But the true test of any model is to see whether or not it depicts all the data, not just some small part of it. In the ideal world, the constants obtained for each vibrational level would be the same each time an experiment is run. Also, the

constants associated with any particular level should be the same no matter which level it is transitioning to. In other words, The B and D coefficient for the $v'' = 1$ level should have the same value for transitions to any v' level. After all, it is the exact same initial state. Unfortunately, this is not the case. Due to the imperfect nature of our data collection, there is some uncertainty in the actual position of the transitional lines.

The best way to deal with this situation when using the term value approach is to attempt a global fit to all the data available about a particular vibrational level. In other words, if the rotational constants of $v'' = 1$ are desired, then every vibrational band involving this level should be used. In this experiment, transitions were seen from $v = 1$ in the ground state to $v = 10$ to 32 in the B state. Thus, there were 23 sets of values that could be used to obtain the $R(J-1) - P(J+1)$ difference. All of these values were then put into Mathematica and a least squares fit was done to this data. The results of this calculation are also displayed in Table 1. Since the original vibrational band of interest also included $v' = 13$, the four different transitions to this band that were observed ($v'' = 0-3$) were used to find a set of $R(J) - P(J)$ differences. The global fit of this data is also displayed in Table 6.1.

As already mentioned, the true test of a model is the accuracy to which it represents the data. As can be easily seen in Fig. 6.2 (on the next page), the global fit numbers are a poor representation at best. Again, this is a graph of the difference of the observed data with respect to the calculated values plotted against the lower state rotational quantum number. At low to moderate J , the model is not too bad. But at high

J it falls off terribly. Recall that in the rotational energy equation there is a J to the fourth dependence of the rotational distortion term. This is the highest order term in the selected representation. Thus, it is reasonable to conclude there is either some error in the value calculated for D_v or an H_v term is needed.

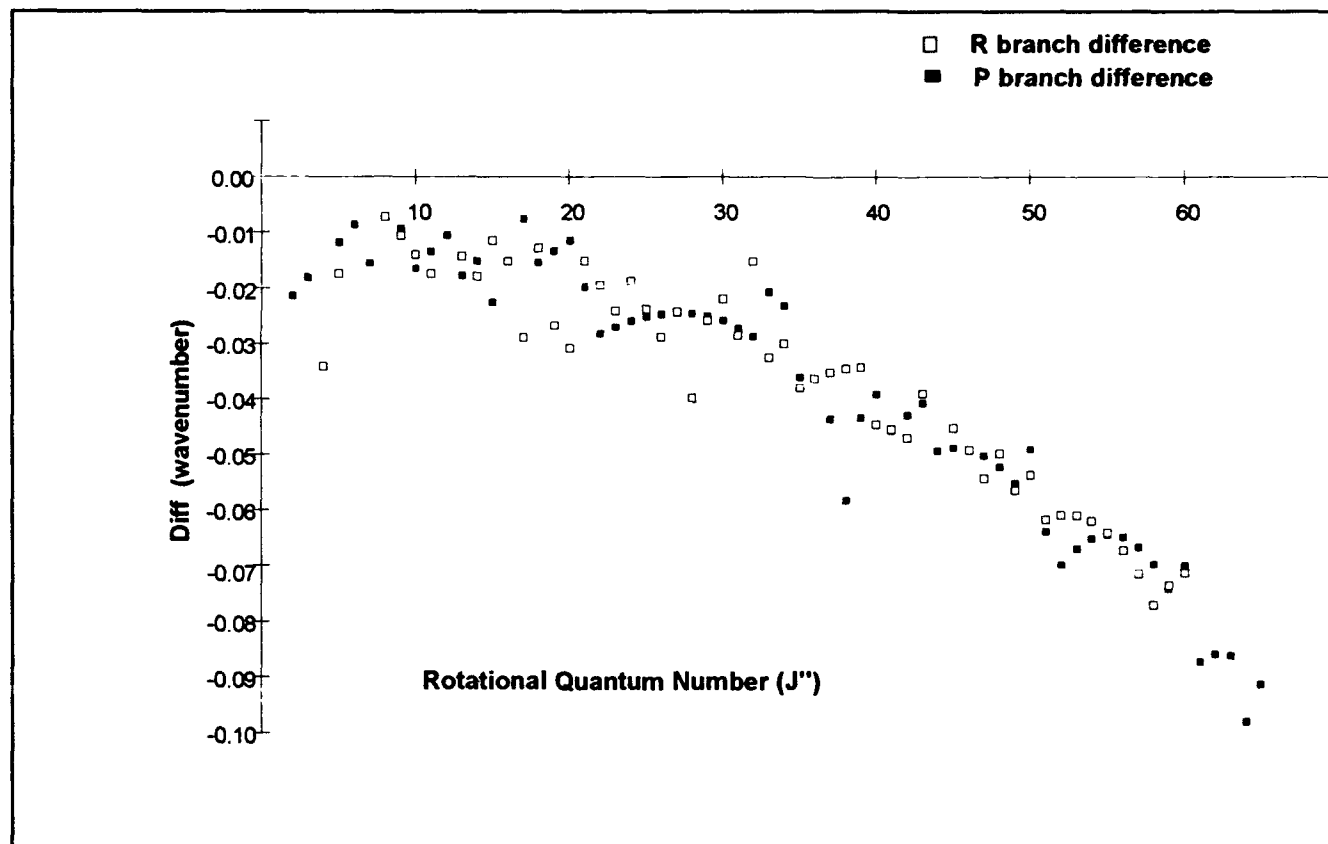


Figure 6.2 Graph of difference in observed value for rotational transition from calculated term value [$v(\text{observed}) - v(\text{calc})$] for global fit plotted against lower state rotational quantum number J'' for $v''=1$ to $v'=13$ band

This is just one example from the data analyzed. Other bands showed the same trend in the higher rotational quantum numbers. Obviously, if the results obtained from this method are unable to reproduce the data to within the resolution of the instrumentation, further refinement of the coefficients is warranted. We have gone as

far as we can with this particular method and have achieved unacceptable results. Thus, a different way of analyzing the data was investigated. Also, it is important to note, the term value approach has provided us with no information on the location of the band origin. This is information that can be easily found in the next method discussed.

Direct Approach

There is another way of looking at each vibrational band that will provide additional information about the energy within the molecule. This approach is called the direct method. This name is derived from the fact that a direct fit using the actual observed values of the wavenumbers will be accomplished on each vibrational band, band by band.

The task at hand is to be able to adequately represent the data in a single equation. By returning to the equations representing the R and P branch transitions, we see they are of different forms. It is possible to fit either the R or P branch data to its appropriate equation to obtain the rotational constants, but this has the drawback of effectively ignoring half the data available. To fit all the data about a particular band to a single equation, we must first come up with the functional form of that equation.

To understand how this will be accomplished, we need to first take a closer look at the two relevant equations. Recall that in an R branch transition, $J' = J'' + 1$, and in a P branch, $J' = J'' - 1$. Schematically, this can be represented by Fig. 6.3. The lowest

value of the rotational quantum number (J) for the upper and lower states is zero. Thus, as Fig. 6.3 shows, the smallest value of J'' in the R branch is zero, while in the P branch it is 1. Furthermore, as the figure shows, these transitions both progress outward from some specific origin. This is where we are able to obtain the equation necessary to analyze the data.

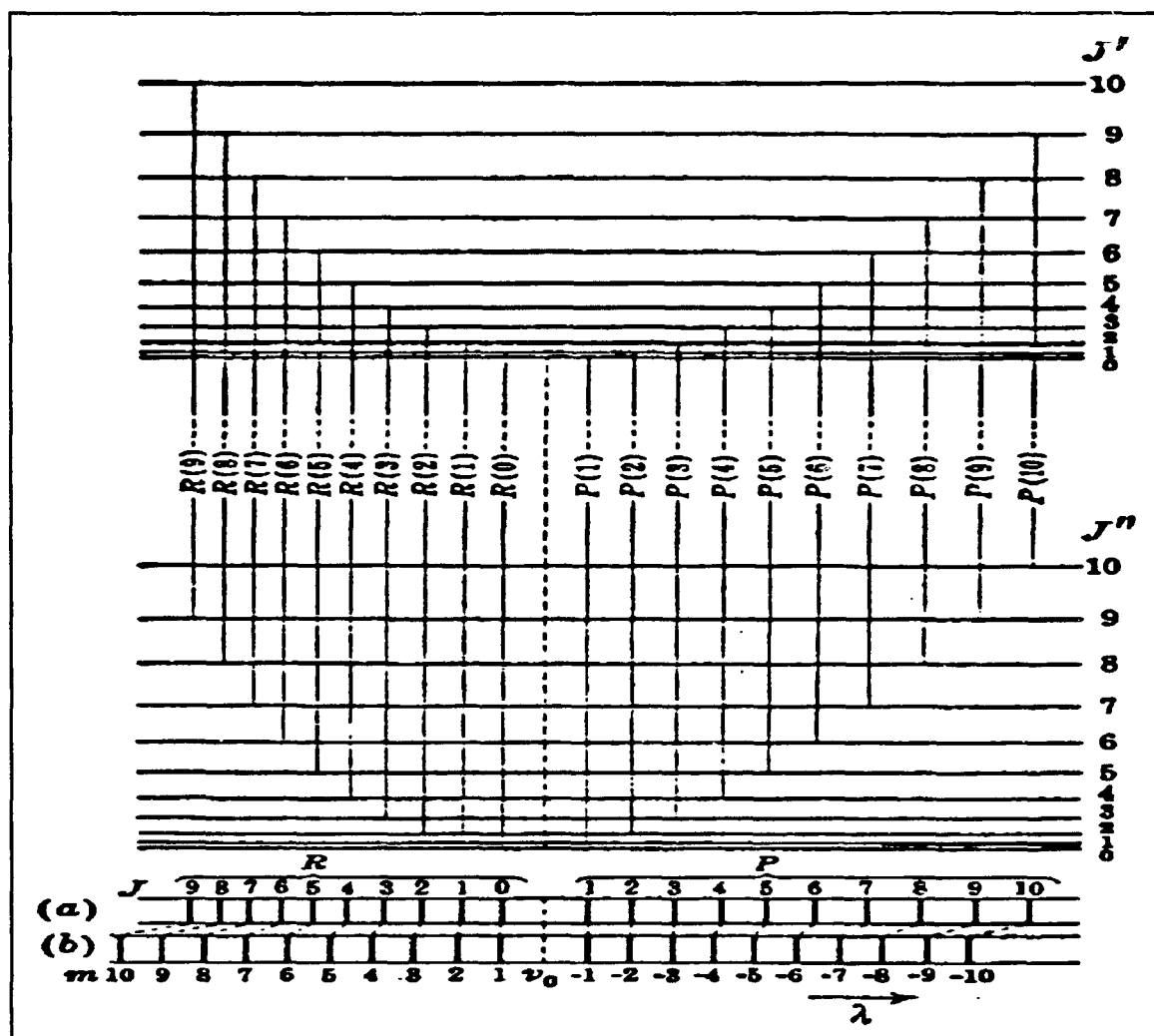


Figure 6.3 Energy level diagram of the fine structure of a Rotation-Vibration band. The *a* line is the normal *R* and *P* numbering, while the *b* line is the *m* equation numbering [5:112]

We will employ a change of variable technique to modify both the R and P branch equations. For the R branch, let $m = J + 1$, and for the P branch let $m = -J$. It can then be easily verified that both branches can be represented by the equation

$$\nu = \nu_0 + (B_v' + B_v'')m + (B_v' - B_v'' - D_v' + D_v'')m^2 - 2(D_v' + D_v'')m^3 - (D_v' - D_v'')m^4 \quad (6.6)$$

where ν is the wavelength of the transition, and ν_0 is the sum of all the vibrational and electronic energy terms. Thus, we now have a single series of lines for which there is a missing line at $m = 0$ (see Fig. 6.3). This missing line, which corresponds to $\nu = \nu_0$, is called the zero line. It corresponds to the forbidden transition between the upper and lower $J = 0$ levels. But more importantly, it is also called the band origin. Thus, where the term value approach did not allow us to calculate the vibrational energy of the bandhead, it has fallen out as a natural consequence of the direct approach.

Now that there is a new equation to use, it is time to apply it to the data at hand. For example purposes, we will go back to the same $v'' = 1$ to $v' = 13$ transition we discussed in the term value approach. When the direct fit is applied to this band, the coefficients contained in Table 6.2 are obtained. Upon comparison with the term value approach, we see there is close agreement on the coefficients obtained for the single band fit. The second value in the table comes from averaging the coefficients obtained for each time either the $v'' = 1$ or $v' = 13$ level was used in a direct fit. Here we see good agreement with the global term value approach on the B_v term, but there is a fair bit of disagreement on the rotational distortion term. Fig. 6.4 and Fig. 6.5 are comparisons

Table 6.2 Table showing the B and D values calculated for the $v''=1$ to $v'=13$ band by using the direct method on a single band and by averaging all like coefficients to obtain a single value

	$10^2 B_v (cm^{-1})$		$10^8 D_v (cm^{-1})$	
	Single Band	Average	Single Band	Average
$v = 13$	5.1610	5.1623	4.8321	5.0221
$v' = 1$	8.1597	8.1627	1.8335	2.1808
	std dev < 0.0016		std dev < 0.40	

of how each set of these parameters fit the data. Once again, these graphs are plots of the residuals of the observed wavelengths with respect to their predicted values plotted against the lower state rotational quantum number.

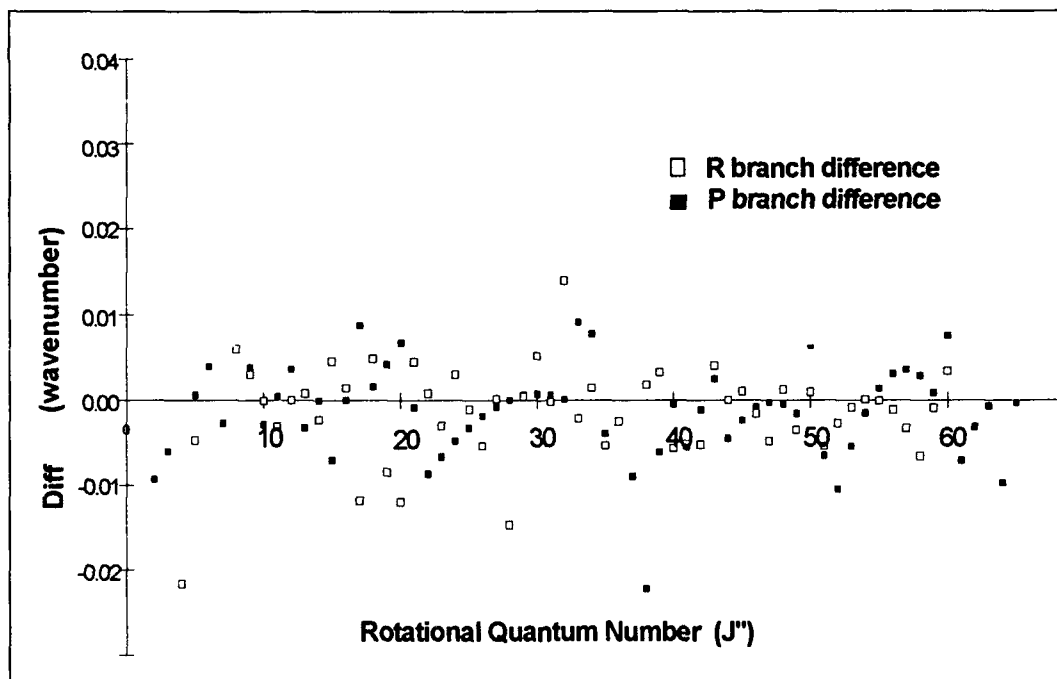


Figure 6.4 Differences in Direct fit on the $v''=1$ to $v'=13$ band

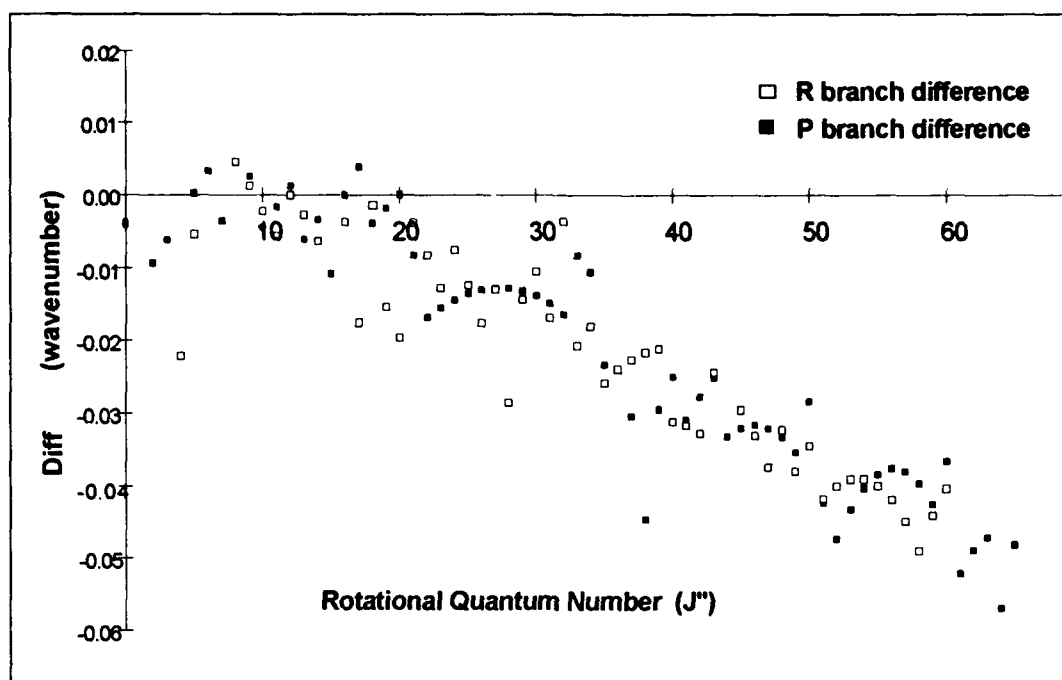


Figure 6.5 Differences in the $v''=1$ to $v'=13$ band using the direct method on all bands and averaging the Coefficients

The single band direct fit is able to recreate the data very efficiently. Also, this time the data is centered about zero. This is because the direct fit was able to provide the location of the band origin. It is interesting to note that the differences observed in this graph are for the most part located within ± 0.01 cm⁻¹ of the zero reference line. Due to the fact the resolution on the spectrometer was 0.02 cm⁻¹ we can feel confident the direct approach applied to a single band is indeed an accurate portrayal of the data.

But again, we run into a problem trying to accurately represent all the transitions that were observed. The fit to the data using the averaged values is poor compared to the direct fit of a single band. This trend was apparent in all vibrational bands. Thus, we are once again forced to conclude that there is a problem in our solution. This problem could come from one of two directions. Either an H_v term is necessary, or

there is some inherent problem with the method we are trying to employ. The former hypothesis is easily tested. The result was that an H_v term did not improve the fit of the data. Thus, we are forced to improve our methods of trying to fit an equation to the data.

Global Least Squares Fit

Part of the problem with the previous two methods is that all the coefficients are interrelated. It is not possible to remove the effects that one band has on all the other bands when trying to find the best parameters to fit the data. Thus, as in the representative band discussed already, the best coefficient for $v'=13$ is different depending on what initial state we are starting from. Ideally, this should not be case, but as mentioned earlier, we have imperfect methods for obtaining our data, and it is now our task to come up with a way to deal with this situation.

The method that was employed to overcome the handicaps of the term value and direct fit methods was to attempt a global least squares fit to the data. The methodology behind this is simple and straightforward.

First, a best guess set of values for all the B_v 's, D_v 's and band origins were collected. These values were the average values that were obtained from the direct method applied to all the data. The assumption is made that none of the values are such that they represent the best fit to the data at hand. The purpose here is to come up with a set of coefficients that represent a better fit to the data. But, first the question

must be asked as to what represents a better fit. It was decided that a better fit was one that minimized the sum of the squared errors from the observed values.

A squared error for a single transition is defined as follows:

$$(Diff)^2 = (\nu_{observed} - \nu_{predicted})^2 \quad (6.7)$$

where $\nu(\text{predicted})$ is the wavelength of the transition predicted from the assumed coefficients. This difference was calculated for each and every transition observed (over 7000). These difference were summed together to give a single value. Since the assumption is made that the initial rotational constants are not ideal, there must be some set of number for which this sum can be made a minimum. This will happen because as the best fit numbers are found, the predicted values will match closer and closer with the observed values. As these two values converge, there difference gets smaller and smaller. Thus, there is less and less to add to the sum, and we eventually find the Least Squared Error.

To find these best fit coefficients, the sum of the squared errors (SSE) was first calculated. Then, exactly one coefficient was varied by a small amount, and the SSE was recalculated. If the new SSE was bigger, the assumption was made that the coefficient was being changed in the wrong direction. This particular parameter was then changed in the other direction, and the SSE was recalculated. This process of changing the designated coefficient was continued as long as the SSE continued to decrease. Once this was no longer possible, it was assumed the coefficient was at its current best fit value. The whole process of varying a parameter was then started all

over again on a new coefficient. This was continued until all coefficients had been examined.

After varying all coefficients one time, it is assumed the first coefficients to be varied probably needed further refinement. After all, numerous parameters had been changed since they were optimized. Thus, the whole process of varying each parameter was started over. This loop was continued as long as there was significant reduction in the value for the SSE. The computer program written to accomplish this task required three loops through this process to optimize the coefficients.

In order to better appreciate the effectiveness of this computer program, the standard error (STE) was calculated. For the purposes of this paper, STE is defined by the equation

$$STE = \sqrt{SSE/N} \quad (6.8)$$

where SSE is as defined previously and N is the number of data points (7749 transitions for this experiment). Thus, standard error gives an approximate order of magnitude of each calculated value from its observed value. The initial value for SSE while using the averaged coefficients was 0.0198 cm^{-1} . After three loops through the computer program this value had dropped to 0.0077 cm^{-1} . Thus, a better fit has been accomplished. Tables 6.3 and 6.4 contain a comparison of the rotational coefficients obtained using the least squared error approach with the coefficients obtained by Barrow.

Table 6.3 Summary of the Rotational Constants (cm^{-1}) for the $X^1\Sigma_g^+$ state of $^{79}\text{Br}_2$

^(a) Barrow's values for D are calculated from RKR procedures

$X^1\Sigma_g^+$	$10^2 B_v$		$10^8 D_v^{(a)}$	
v	AFIT	Barrow	AFIT	Barrow
0	8.1946	8.1947	2.1213	2.097
1	8.1626	8.1627	2.1813	2.108
2	8.1305	8.1304	2.2619	2.116
3	8.0972	8.0979	2.0869	2.135

Table 6.4 Summary of the Rotational constants (cm^{-1}) for the $B^3\Pi(0_v^+)$ state $^{79}\text{Br}_2$

$B^3\Pi(0_v^+)$	$10^2 B_v$		$10^8 D_v$	
v	AFIT	Barrow	AFIT	Barrow
10	5.3674	5.3687	4.4341	4.40
11	5.3021	5.3039	4.8216	5.00
12	5.2344	5.2363	5.0933	5.20
13	5.1636	5.1644	5.1066	5.10
14	5.0925	5.0927	5.6597	
15	5.0180	5.0181	5.9398	
16	4.9407	4.9399	6.0445	5.50
17	4.8619	4.8626	6.4441	6.24
18	4.7813	4.7801	7.0000	6.49
19	4.6970	4.6979	7.1279	7.36
20	4.6109	4.6122	7.6625	7.74
21	4.5246	4.5230	8.7204	8.09
22	4.4329	4.4338	8.9753	8.98
23	4.3401	4.3404	9.6072	9.26
24	4.2438	4.2426	10.0580	9.63
25	4.1451	4.1453	10.5060	9.89
26	4.0470	4.0451	11.5610	10.96
27	3.9461	3.9444	12.6240	12.29
28	3.8405	3.8392	12.9260	12.30
29	3.7361	3.7338	14.2000	13.56
30	3.6293	3.6283	15.4110	15.08
31	3.5170	3.5184	15.6300	15.59
32	3.4069	3.4065	17.0330	16.81
33	3.2965	3.2944	18.8710	18.12

For the most part, these values are in close agreement with values reported by Barrow. The largest deviations tend to be in the values arrived at for D_v . This is true for both the X and the B state. As a quick comparison to show that these global fit numbers are indeed recreating the data, we will revisit the $v''=1$ to $v'=13$ band that has been used as an example earlier in this chapter. When the rotational coefficients listed above are put in the Dunham expansion and the residuals of the $v''=1$ to $v'=13$ rotational transitions are plotted as a function of the lower state rotational quantum number, the result is seen in Fig. 6.6.

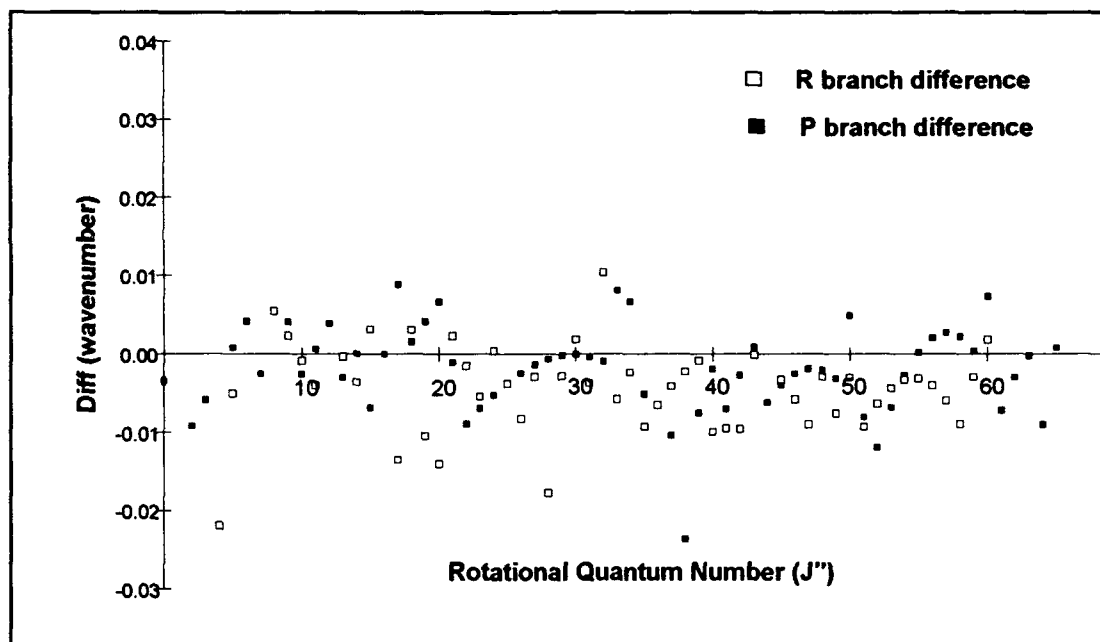


Figure 6.6 Plot of the residuals of the $v''=1$ to $v'=13$ band when global fit rotational coefficients are used

This figure shows a marked improvement over the other two attempts at a global fit. Virtually all residuals are located in a band that is only 0.02 cm^{-1} wide. Considering this is the resolution of the spectrometer used, attempts at a tighter fit would be pointless.

Other bands observed had the same tendency for small residuals. Thus, we can now assume that for the data taken in this experiment, a two term expansion of the rotational part of the Dunham expansion is adequate to represent the data.

As far as the actual values that were obtained, all of them except one trend very nicely with what is predicted by theory. All the B_v terms are decreasing as the vibration level increases. As this term is related to the actual rotation of the molecule, this is expected. At higher vibration levels, the average moment of inertia of the system is larger, and this will tend to decrease the rotational energy. But, the increasing vibrations of the molecule have an opposite effect on the distortion terms. All of them, except for the $v''=4$ D_v term, are increasing as the vibrational level increases. We would expect this term to get larger. As the vibration of the molecule increases, the average separation of the nuclei is greater. Thus, since this term is subtracted from the rotational energy, we would expect there to be a larger correction to the rotational energy because of the increased average moment of inertia. Thus, the one anomalous value of D_v is probably in error. After examining the data, a reason for this could not be found.

Rotational Expansion

As was mentioned in the theory section of this paper, the rotational coefficients are coupled to the vibration level of the molecule. This is because of the non-rigid rotor process within the motion of the system. What that means at this point is that we are still not finished with the rotational coefficients. B_v and D_v can each be represented as

a polynomial expansion in $(v + 1/2)$. If we can find the correct coefficients on these expansions, then we can represent the rotational terms of all vibration levels mathematically.

To accomplish this is a relatively simple process. A least squares fit was accomplished on both B_v and D_v for each electronic state. The goal of this fitting process was to find the number of terms necessary to accurately represent the data. Due to the fact diatomic bromine has an anharmonic potential, no expansions with less than three term were considered. Also, since there were only four levels observed in the X state, it would have been pointless to consider more terms than this for its expansion. The following paragraphs will present a discussion of how the appropriate number of terms was derived.

For starters, the final solution to the question being asked was that three terms were necessary for the B_v expansions and four terms for D_v in the X state and five terms were necessary for both expansions in the B state. Using these coefficients, the final STE was 0.0086 cm^{-1} . This compares very favorably with the value of 0.0077 cm^{-1} arrived at by using just the rotational terms. Also, the largest residual calculated with these coefficients was approximately 0.05 cm^{-1} . This value appears to be a little large for comfort. As this value showed up several times while different numbers of coefficients were tested, it is assumed this particular measurement was probably in error. As far as the X state goes, the D_v term was the easiest to determine the number of coefficients necessary. As previously stated, the $v''=3$ term did not trend as

expected. Accordingly, it was necessary to use four terms in the expansion to completely specify the system. Thus, reproduction of the exact D_v terms was assured.

There were only two choices regarding the number of terms for the X state B_v . Either use three or four terms. The choice here made little difference on the solution. When four terms were used, the value of the STE only decreased to 0.0083 cm^{-1} . The maximum residual was still approximately 0.05 cm^{-1} . The decision to use the three term expansion was prompted by the standard deviation of the coefficients from the least squares fit. For the four term fit, the deviation on the fourth coefficient was larger than the coefficient itself. Because this term could not be determined with any certainty and because the change in the STE was minuscule, the three term fit was accepted.

As for the B state, the same analysis was used. There was a marked improvement in the STE when the B_v expansion went from four to five terms. With four terms, the STE jumped all the way to 0.02 cm^{-1} and the maximum residual increased to 0.08 cm^{-1} . The standard deviations were of approximately the same order of magnitude with respect to their corresponding coefficient. As for the D_v expansion, there was not a clear best choice. As the number of terms was varied, the first term in the expansion varied wildly. Thus, it was basically a gut feel that made the decision to use five terms. To illustrate this point is the fact that the standard deviations in this expansion were all of the same order of magnitude as the actual coefficients.

The final solution is seen in Table 6.5. For ease in writing the coefficients, they will be labeled with a lower case number to designate to which expansion they belong.

Also, they will be given a number to correspond to what power of $(v+1/2)$ they are coupled to. Remember, the sign on the second term is negative.

Table 6.5 Rotational Molecular Constants (cm^{-1})
for the 79-79 isotope of Diatomic Bromine

	$B^3\Pi(0_u^+)$	$X^1\Sigma_g^+$
b1	5.97638 +/- 0.02 E-02	8.21020 +/- 0.00 E-02
b2	5.42374 +/- 0.45 E-04	3.11300 +/- 0.05 E-04
b3	1.47381 +/- 0.33 E-07	-3.25000 +/- 1.22 E-06
b4	-4.05763 +/- 1.04 E-07	
b5	5.12229 +/- 1.18 E-09	
d1	6.07526 +/- 6.14 E-08	2.18534 +/- 0.00 E -08
d2	5.74659 +/- 1.26 E-09	2.25292 +/- 0.00 E -09
d3	5.53281 +/- 6.61 E-07	2.17450 +/- 0.00 E -09
d4	-1.62072 +/- 2.93 E-11	-4.60333 +/- 0.00 E -10
d5	2.42843 +/- 3.32 E-13	

Vibrational Bandhead analysis

Now that we know the coefficients to adequately represent the rotational spectrum, it is time to turn to the locations of the vibrational bandheads. As a brief reminder, let's first look at the equation that expresses these locations. It is

$$\nu_0 = T_e' + G_v' - [T_e'' + G_v''] \quad (6.9)$$

where ν_0 is the band origin, and for the case of the ground state electronic energy, $T_e'' = 0.0$. As in the case of the equations used to expand the rotational coefficients, the

values for G_v are also polynomials expanded in terms of $(v + 1/2)$. Our goal, is to come up with the coefficients that will allow these polynomial expansions to fully represent the data.

The data that is to be represented is contained in Table 6.6. This table contains the

Table 6.6 *Summary of vibrational Molecular constants (cm^{-1}) as derived in this study and as reported by Barrow.*

	Present Work	Barrow
	$T(v, J=0)$	$T(v, J=0)$
v		
10	17308.670	17308.65
11	17436.870	17436.89
12	17561.160	17561.14
13	17681.500	17681.50
14	17797.838	17797.88
15	17910.135	17910.18
16	18018.355	18018.37
17	18122.480	18122.45
18	18222.480	18222.46
19	18318.344	18318.33
20	18410.078	18410.07
21	18497.673	18497.66
22	18581.150	18581.13
23	18660.530	18660.52
24	18735.866	18735.86
25	18807.190	18807.20
26	18874.560	18874.56
27	18938.057	18938.04
28	18997.747	18997.73
29	19053.722	19053.71
30	19106.080	19106.05
31	19154.920	19154.90
32	19200.337	19200.32
33	19242.460	19242.44
v'		
0	0.000	0.00
1	323.148	323.16
2	644.121	644.14
3	962.907	962.94

values of $T(v, J=0)$, which is the vibrational term value relative to the X state ($v''=0, J=0$). For the ground state, $G(v)=T(v, J=0)+ 162.39 \text{ cm}^{-1}$, and for the excited state $G(v) = T(v, J=0) - 15470.08 \text{ cm}^{-1}$. These values will reproduce all band origins to within $\pm 0.01 \text{ cm}^{-1}$. These values are compared with those of Barrow's work derived in a similar manner.

To find the coefficients of the expansion, it is possible to first use a term value approach to isolate either the upper or lower state coefficients. But, as can be recalled from earlier in this section, this method does not always produce the best fit parameters. Suffice it to say that this method was attempted on the vibrational bandheads and it met with unacceptable results. As was already pointed out, one way of dealing with a situation like this is to try a global least squares fit on the data. With minor modifications, the computer program written to analyze the rotational results could be used for the vibrational analysis. It was unknown how many terms were needed in each expansion to adequately model the data. After some trial and error on the computer program, it was possible to reproduce all vibrational band origins to within 0.03 cm^{-1} by using five terms on the expansion of the excited state and three terms in the expansion of the ground state. The use of these coefficients degraded the accuracy of the model somewhat. The STE was 0.0159 cm^{-1} when these coefficients were used. An attempt at a fourth term in the X state expansion gave results no better than those previously mentioned. In contrast, fewer terms on the excited state expansion reduced the accuracy of the model even further, while trying to add a sixth term made the model go unstable (i.e. the terms experienced a large variation from

previous value). The terms that were derived are listed in Table 6.7. The convention on these terms is similar to the convention used in Table 6.5. This time, the common term is listed as a lower case g.

Table 6.7 *Electronic and Vibrational Constants (cm^{-1})
to fit the vibrational levels $v''=0-3$ with $v'=10-33$*

	$\text{B}^3\Pi(0_v^+)$	$\text{X}^1\Sigma_g^+$
T	15748.886	0
g1	165.05772	325.32668
g2	1.35975	1.09042
g3	-2.27005 E -02	2.52659 E -04
g4	2.19041 E -04	
g5	1.60489 E -06	

It needs to be pointed out that just as in Barrow's previous work, this effort was unable to reproduce the vibration band origins to within 0.02 cm^{-1} for the B state levels greater than ten. One possible explanation for this deals with the crossing of the repulsive $^1\Pi$ state. At vibration levels greater than four in the excited state, An interaction begins between the bound and repulsive states. Thus, the anharmonic nature of the bound state is disturbed. The model being used in these calculations does not take this into effect. Thus, it is reasonable to assume that these interactions are part of the reason the model is not working properly.

VII. Discussions and Recommendations for Future Work

Introduction

This final section discusses the results achieved and suggest possible future efforts that could be made in this area. As the results of the different fit models have already been presented, it will not be given again here. Instead, this discussion will focus on the meaning of what's been observed.

Discussion

The original aim of this work was to derive a set of molecular constants that when substituted back into the Dunham Equation would fully represent the data. This goal was at least partially successful. The rotational analysis provided a better fit to the data than was previously seen in the work by Barrow. A good example of this can be seen in Figs. 7.1 and 7.2. These figure are plots of the residuals of the $v''=2$ to $v'=18$ absorption band using first Barrow's coefficients, and then the best fit numbers obtained in this research.

In the graph plotted with Barrow's data, the high rotational numbers have a trend away from a straight line. The trend is growing more pronounced as J gets larger. This trend was evident in all vibrational bands observed. Generally speaking, the move away from a zero reference line began around $J''=50$ in all bands. The cause of this could come from one of two areas. Either the data is in error, or the model used by

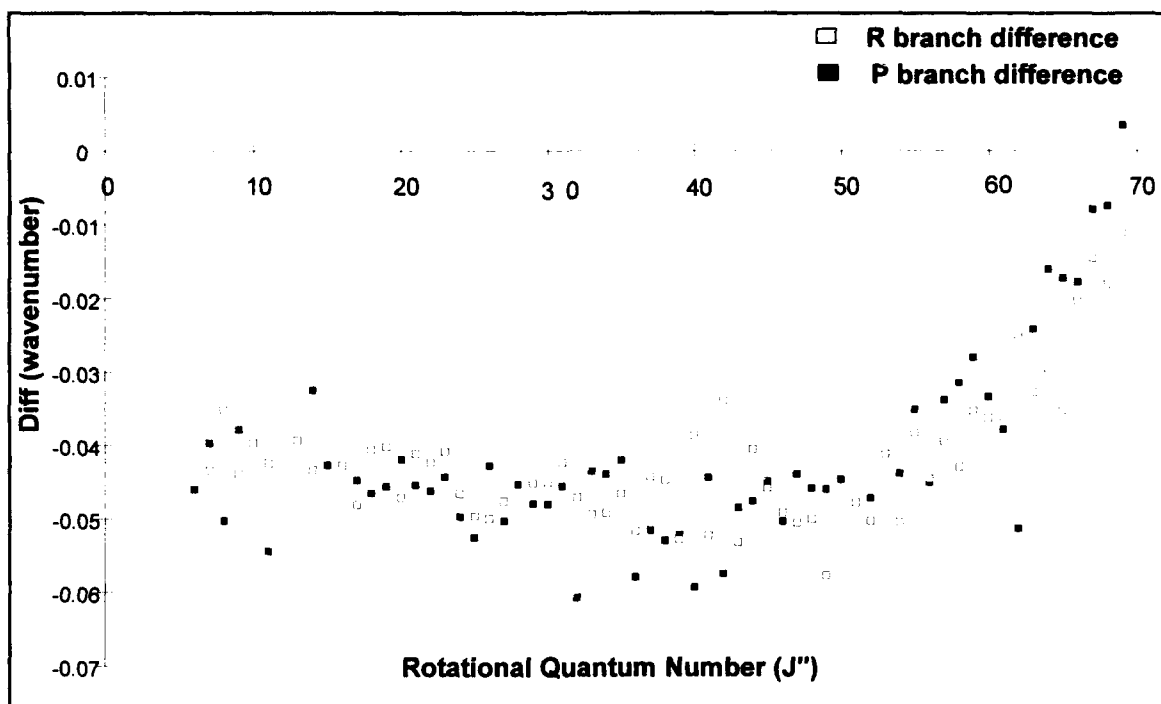


Figure 7.1 Residuals of $v''=2$ to $v'=18$ band using Barrows constants.

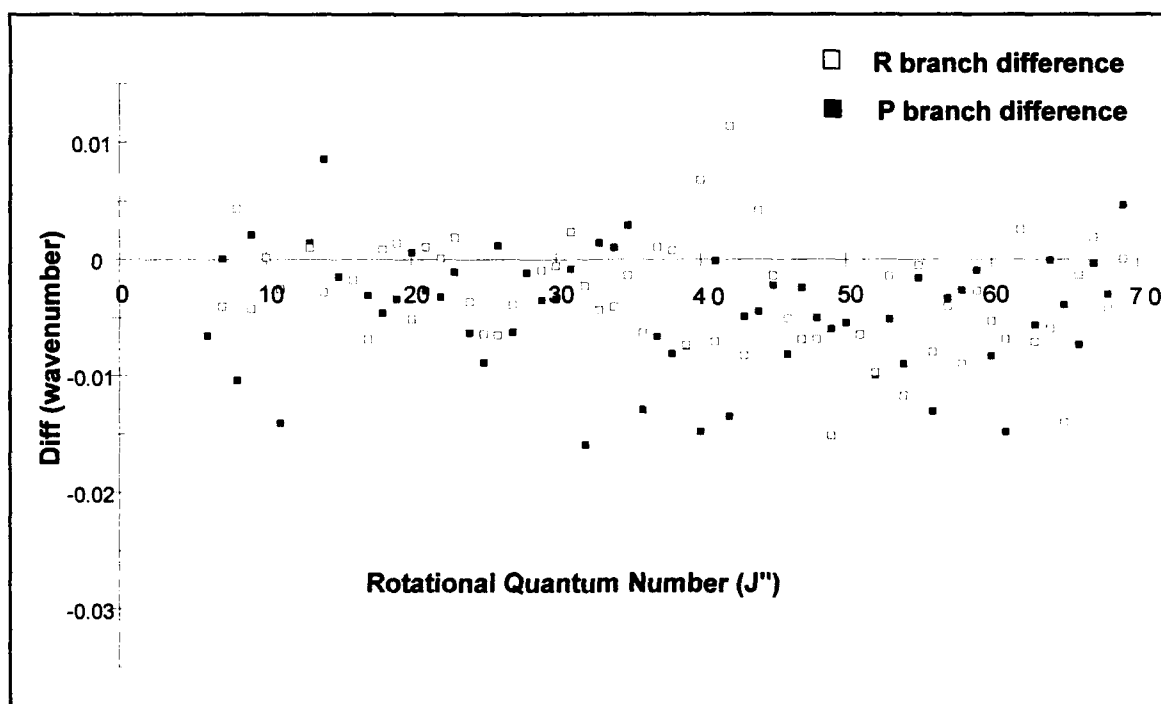


Figure 7.2 Plot of the residuals of the $v''=2$ to $v'=18$ vibrational band with best fit coefficients from this study.

Barrow was inappropriate for high J . Since the same general behavior was seen in all bands, this leads to the conclusion that refinement of the rotational coefficients is warranted. The cause of the inferior fit is probably due to the earlier work seeing fewer rotational transitions than was seen in this work. One other potential problem area arises because Barrow's B state rotational coefficients, derived in a direct fit process, were calculated based off constrained values of the ground state rotational coefficients. By constraining these two terms, he effectively limited the ability of his model to reach a minimum error.

The residuals when the data from this effort was used are all tightly clumped about zero. This is an indication that the correct model is being used on the data as observed. The plot in Fig 7.2 was done using the term value for the vibrational bands and not the Dunham Expansion calculation. For this band, it would have made no difference. This was one of the vibrational bands fit to less than 0.01 cm^{-1} of its observed value. If it had been one the bands that could not be matched as closely, the spread of the data would not have changed, just its position the plot, indicating a systematic error.

Another observation of the plot with Barrow's coefficients is that the residuals do not start out near zero. This was another trend that was seen in most of the vibrational bands. Since the residuals stay constant all the way out to $J'' = 50$, the conclusion must be reached that there is some discrepancy between the actual location of the vibrational bandhead and its location as predicted Barrow's work. By using the results

of the direct approach on each specific band, more accurate values of the vibration bandhead locations have been found.

As was pointed out in Chapter VI, the most accurate way to locate the vibrational bandheads is by direct use of the different vibration levels origins. The vibrational expansion induces error into the equation. This occurs because the imperfect nature of the polynomial fitting process is more pronounced for calculating these bandheads.

The question should be raised as to whether or not the fitting routine used on the vibration levels was actually performing correctly. This routine was applied to Barrow's data over the ranges he said he could achieve a good fit. All the coefficients derived agreed with Barrow's to less than 0.001 cm^{-1} . The question might be raised as to whether Barrow's coefficients, or the ones achieved in this research are actually more correct. When the coefficients from this research were extrapolated back to the $v''=0$ to $v'=0$ bandhead, there was almost an 8.0 cm^{-1} deviation as compared to the data collected by Barrow. The only conclusion that can be reached here is that vibrational levels less than $v' = 10$ need to be observed in order to attempt an accurate fit.

In summary, it can be concluded from this research that refinement of the rotational coefficients is warranted. A superior fit of rotational transitions has been achieved. Presently, there is not enough data available make any conclusion about the vibrational levels or energy spacing.

Recommendations

Several tasks can be accomplished to provide better molecular constants for the $B^3\Pi(0_u^+)$ to $X^1\Sigma_g^+$ system of $^{79}\text{Br}^{79}\text{Br}$. First, several test runs should be done to validate the results achieved here. After this, absorption out of more of the ground state vibration levels and to more of the B state levels should be observed. Currently, a 1.5 meter absorption cell has been built to the same specifications as the 25 cm cell used in this research. In the ground state of bromine, each successive vibration level contains approximately one fifth as many particle as the previous level. Since this new cell is six times as long, it will allow access to at least one, and possibly two more ground state vibration levels. This assumption is made because bandheads for both $v'' = 4,5$ were identified but not accurately located.

Another way to increase the population in the ground state levels is by heating the sample. The Boltzmann distribution of the energy level populations as a function of temperature show that when the sample is heated to approximately 400K, there is now sufficient population in the vibrational levels to accurately observe two to three additional levels for the 1.5 m cell. This would take the observable ground state vibrational levels to somewhere between six and eight. If the cell can handle an additional 100 K, then vibration levels up to $v''=10$ are achievable. These temperature values compare favorably to the work done by Coxon [3] who was able to observe $v''=8$ at 520 K when using a 55 cm cell. Accessing these levels provides another benefit. Due to the Franck-Condon principle, these higher v'' levels are necessary to observe

transitions to the lower v' levels. These efforts would provide the data necessary to attempt a global fit on the data using a much larger database.

Bibliography

1. Barrow, R.F., T.C. Clark, J. A. Coxon, K.K. Yee. "The $B^3\Pi(0_v^+) - X^1\Sigma_g^+$ System of Br_2 : Rotational Analysis, Franck-Condon Factors, and Long Range Potential in the $B^3\Pi(0_v^+)$ State," *Journal of Molecular Spectroscopy*, 51:428-449 (1974)
2. Bell, Robert John. *Introductory Fourier Transform Spectroscopy*, New York: Academic Press, Inc., 1972.
3. Coxon, J.A. "The $B^3\Pi(0_v^+) \leftarrow X^1\Sigma_g^+$ System of $^{79}Br^{79}Br$," *Journal of Molecular Spectroscopy*, 37:39-62 (1971).
4. Gerstenkorn, S., and P.Luc, *Atlas Du Spectre D'Absorption De La Molécule D'Iodide*, Paris:Centre National de la Recherche Scientifique, 1978.
5. Graybeal, Jack D. *Molecular Spectroscopy*, McGraw-Hill, Inc., 1988.
6. Herzberg, Gerhard, *Molecular Spectra and Molecular Structure*, Litton Educational Publishing, Inc., 1950.
7. Holmberg, Courtney D. "Spectroscopic and Vibrational Transfer Studies in Molecular Bromine," Dissertation, Not Yet Published (1993).
8. Horsley, J.A, and R.F. Barrow. "Absorption Spectrum of Bromine from 6200 to 5100 Angstroms," *Transaction of the Faraday Society*, 63:32-38 (1967).

Vita

Captain Robert E. Franklin was born April 1, 1964 in Dallas, Texas. He graduated from Midway High School in Waco, Texas in 1982. In June of 1986 he graduated from the United States Air Force Academy with a Bachelor of Science Degree in Physics, and then attended Undergraduate Navigator Training at Mather AFB, California. Upon earning his wings in May of 1987, he was assigned to the 67th Tactical Reconnaissance Wing, Bergstrom AFB, Texas, where he became a Mission Ready RF-4C Weapons System Officer (WSO). While stationed at Bergstrom, he was upgraded as an Instructor WSO and served as the Chief of the Maintenance Quality Assurance Division where he was directly responsible for the maintenance standards on 30 wing aircraft. Before leaving Bergstrom, he accumulated over 1000 hours of flight time in the Phantom II, including 32 sorties and 96.5 hours of combat time in the Persian Gulf War. He then entered the School of Engineering, Air Force Institute of Technology, in June of 1992.

Rob Married Sheila Gay of Idaho Falls, Idaho in February of 1990.

Permanent Address:	9012 Lark Dr.
	Waco, Texas 76712

REPORT DOCUMENTATION PAGE			Form Approved OMB No 0704-0188	
<small>Public report no burden for this collection of information. It is estimated that a burden of 1 hour per response, including the time for reviewing existing data sources, gathering and maintaining the data needed, and completing and reviewing the collection of information. Send comments regarding this burden estimate or any other aspect of this collection of information, including suggestions for reducing this burden, to Washington Headquarters Services, Directorate for Information Operations and Reports, 1215 Jefferson Davis Highway, Suite 1204, Arlington, VA 22202-4302, and to the Office of Management and Budget, Paperwork Reduction Project (0704-0186), Washington, DC 20503.</small>				
1. AGENCY USE ONLY (Leave blank)		2. REPORT DATE December 1993		3. REPORT TYPE AND DATES COVERED Master's Thesis
4. TITLE AND SUBTITLE HIGH RESOLUTION FOURIER TRANSFORM ABSORPTION SPECTRUM OF $^{79}\text{Br}_2$ $\text{B}^3\Pi(0_u^+) \leftarrow \text{X}^1\Sigma_g^+$			5. FUNDING NUMBERS	
6. AUTHOR(S) Robert E. Franklin, Captain, USAF				
7. PERFORMING ORGANIZATION NAME(S) AND ADDRESS(ES) Air Force Institute of Technology, WPAFB OH 45433-6583			8. PERFORMING ORGANIZATION REPORT NUMBER AFIT/GAP/ENP/93D-2	
9. SPONSORING/MONITORING AGENCY NAME(S) AND ADDRESS(ES) Dr. Ernie Dorko PL/LID Kirtland AFB, NM 87117-6008			10. SPONSORING/MONITORING AGENCY REPORT NUMBER	
11. SUPPLEMENTARY NOTES				
12a. DISTRIBUTION/AVAILABILITY STATEMENT Approved for public release; distribution unlimited			12b. DISTRIBUTION CODE	
13. ABSTRACT (Maximum 200 words) High Resolution Fourier Transform Spectroscopy has been conducted for the $\text{B}^3\Pi(0_u^+) \leftarrow \text{X}^1\Sigma_g^+$ system of $^{79}\text{Br}_2$. A total of 64 vibrational levels, including $v'' = 0-3$ and $v' = 10-33$, have been observed and assigned. Rotational levels as high as $J=76$ were observed. A global fitting routine has been developed to fit the rotational spectra to the Dunham Expansion. Using B_v and D_v for both the X and B state, rotational transitions were calculated to within 0.02 cm^{-1} . The expansions of these terms required five coefficients for the B state and three coefficients for the X state. Attempts to fit the vibrational spectrum to an equation in terms of $(v+1/2)$ were only accurate to within 0.03 cm^{-1} when five molecular constants were used on the upper level and three were used on the ground state. However, direct calculation of the vibrational energy levels was able to fit all vibrational bandheads to less than 0.02 cm^{-1} . Recommendations are made for attempting a global fit over many more vibrational bands.				
14. SUBJECT TERMS Bromine, interhalogens, Dunham Expansion, spectroscopy			15. NUMBER OF PAGES 68	
			16. PRICE CODE	
17. SECURITY CLASSIFICATION OF REPORT Unclassified	18. SECURITY CLASSIFICATION OF THIS PAGE Unclassified	19. SECURITY CLASSIFICATION OF ABSTRACT Unclassified	20. LIMITATION OF ABSTRACT UL	